Icarus 212 (2011) 790–806

Contents lists available at ScienceDirect

Icarus

journal homepage: www.elsevier.com/locate/icarus

Titan: An exogenic world?

Jeffrey M. Moore [a,*], Robert T. Pappalardo [b]

[a] NASA Ames Research Center, Space Science Division, M/S 245-3, Moffett Field, CA 94035, United States
[b] Jet Propulsion Laboratory, California Institute of Technology, M/S 321-560, Pasadena, CA 91109, United States

ARTICLE INFO

Article history:
Received 4 March 2010
Revised 13 January 2011
Accepted 19 January 2011
Available online 1 February 2011

Keywords:
Saturn, satellites
Titan
Titan, atmosphere
Titan, hydrology
Titan, surface

ABSTRACT

All landforms on Titan that are unambiguously identifiable can be explained by exogenic processes (aeolian, fluvial, impact cratering, and mass wasting). Previous suggestions of endogenically produced cryovolcanic constructs and flows have, without exception, lacked conclusive diagnostic evidence. The modification of sparse recognizable impact craters (themselves exogenic) can be explained by aeolian and fluvial erosion. Tectonic activity could be driven by global thermal evolution or external forcing, rather than by active interior processes. A lack of cryovolcanism would be consistent with geophysical inferences of a relatively quiescent interior: incomplete differentiation, only minor tidal heating, and possibly a lack of internal convection today. Titan might be most akin to Callisto with weather: an endogenically relatively inactive world with a cool interior. We do not aim to disprove the existence of any and all endogenic activity at Titan, nor to provide definitive alternative hypotheses for all landforms, but instead to inject a necessary level of caution into the discussion. The hypothesis of Titan as a predominantly exogenic world can be tested through additional Cassini observations and analyses of putative cryovolcanic features, geophysical and thermal modeling of Titan's interior evolution, modeling of icy satellite landscape evolution that is shaped by exogenic processes alone, and consideration of possible means for supplying Titan's atmospheric constituents that do not rely on cryovolcanism.

Published by Elsevier Inc.

1. Introduction

Following the first flyby of Titan by the Cassini spacecraft in October 2004, there were several published studies reporting on evidence and analysis of icy volcanism, or "cryovolcanism," on Titan, based on data from the Cassini radar and the Visual and Infrared Mapping Spectrometer (VIMS) instruments (Elachi et al., 2005, 2006; Barnes et al., 2006; Stofan et al., 2006; Lopes et al., 2007, 2010; Nelson et al., 2009a,b; Wall et al., 2009; Le Corre et al., 2009; Soderblom et al., 2009; Jaumann et al., 2009a). Cryovolcanism can be defined as "eruptions... that consist of liquid or vapor phases of materials that freeze at temperatures of icy satellite surfaces" (Prockter, 2004). The term "cryovolcanism" can also include the possibility of solid-state (diapiric) emplacement of materials. Cryovolcanism is canonically associated with an icy body that has a warm and active interior (e.g., Schenk and Moore, 1998).

The level of reported certainty of interpretation for cryovolcanic features on Titan ranges from "putative" cryovolcanic domes and flows (Lopes et al., 2007) to assertions of "strong evidence" for active cryovolcanic venting (Nelson et al., 2009a). The cumulative weight of these reports has generally conveyed a sense that evidence for cryovolcanic activity, based on remote sensing observations, is conclusive or nearly so (e.g., Jaumann et al., 2009a; Lopes et al., 2010). The present contribution urges a cautious approach to this issue, given many incidences of equivocal identification of planetary volcanism (see Section 4), combined with the inherent resolution limitations of Titan remote sensing data and the uniqueness of Titan's surface as an icy satellite affected by exogenic processes (i.e., energy for modification is supplied externally to the planetary surface), specifically fluvial (Fig. 1) and aeolian activity (Fig. 2) as well as impact cratering (Fig. 3). Here we do not aim to disprove the existence of any and all endogenic activity on Titan, nor to provide definitive alternative hypotheses for all landforms, but instead to inject a necessary level of caution into the discussion.

In this paper, we will: (Section 2) summarize the challenges of Cassini image interpretation through Titan's atmosphere; (Section 3) briefly review the evidence of various exogenic geological processes that have shaped Titan's surface; (Section 4) consider lessons from the history of the initial phases of planetary geological exploration (of the Moon, Mars, Mercury, and the icy satellites) for certain processes operating on planetary surfaces, and the cautions that can be drawn from those experiences; (Section 5) consider case examples of Titan's features previously argued to be cryovolcanic, which can instead be interpreted as related to other processes, and touch on the issue of tectonism; (Section 6) note that the interpretation of a relatively quiescent Titan interior is consistent with a broad range of geophysical constraints; and

* Corresponding author. Fax: +1 650 604 6779.
E-mail addresses: jeff.moore@nasa.gov (J.M. Moore), robert.pappalardo@jpl.nasa.gov (R.T. Pappalardo).

0019-1035/$ - see front matter Published by Elsevier Inc.
doi:10.1016/j.icarus.2011.01.019

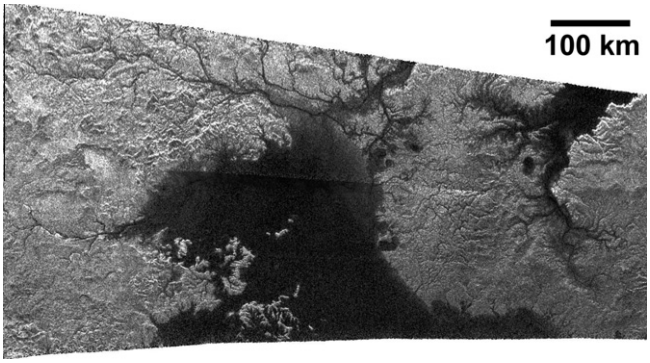

Fig. 1. A landscape of Titan unambiguously dominated by fluvial and lacustrine erosion, transportation and deposition. The scene is centered at 75°N, 260°W (excerpted from Cassini SAR swath T28).

(Section 7) consider the implications for the geological and atmospheric evolution of Titan.

2. Challenges of landform identification on Titan

Geological interpretation of spacecraft images is based on the fundamental recognition of image tone, textures, pattern, shape, size, and relation of associated features (e.g. Ray, 1960). Even under ideal conditions, ~2–3 pixels are required across a high-contrast feature in order to be said to "resolve" that feature (Drury, 2001). The exception to this are lineaments (straight or otherwise), which merely need to return enough energy within their pixels to produce distinctive contrasts along a string of pixels, even if the lineaments themselves are more narrow than a pixel.

Experience with unambiguous volcanic landforms provides diagnostic criteria for their recognition. Volcanic effusion is primarily an accretionary constructive (landform building) process, generally with a negligible erosive role. The criteria for volcanic deposits include recognition of flow fronts, flow textures, identification of source vents, embayment and superposition relationships of the flows over pre-existing surfaces (including earlier flows).

Geological interpretability of planetary landscapes is substantially improved with the addition of topographic information. In all cases, better spatial resolution (both horizontal and vertical) increases interpretability, as long as coverage is appropriate to the scale of features under study. Through an atmosphere as aerosol-laden as Titan's, scattering is a severe limitation to visible and near-infrared imaging, reducing the contrast and effective resolution of optical images. Synthetic Aperture Radar (SAR) images do not have this limitation, but present their own challenges to the geologist, as discussed below.

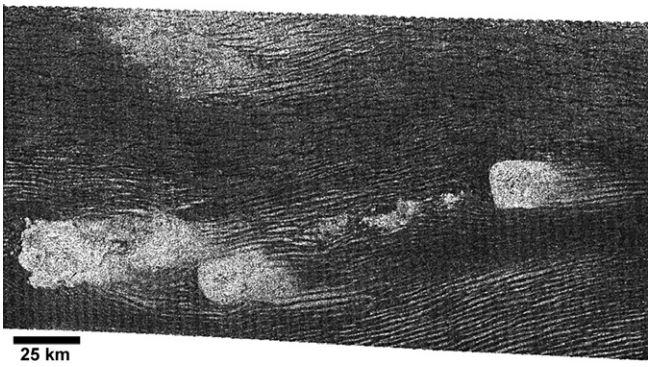

Fig. 2. Unambiguously identifiable Aeolian sand dunes on Titan, surrounding topographic obstacles. The scene is located at 8°N, 44°W (excerpted from Cassini SAR swath T17).

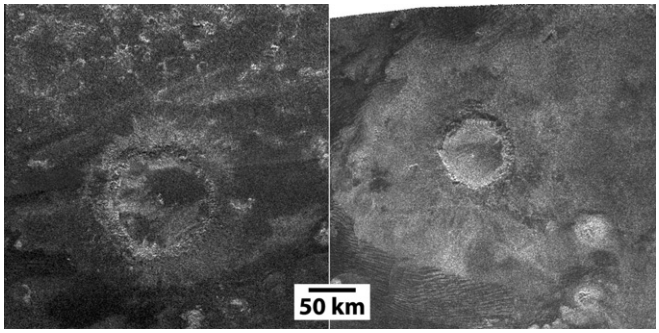

Fig. 3. Examples of unambiguously recognizable impact craters on Titan. Given their size, shape, arrangement, and textures of component landforms (e.g., the central peak and radial external ejecta) and the relative lack of modification by erosion make their interpretation uncontroversial. The crater on the right is Sinlap (diameter 79 km) located 11°N, 16°W (excerpted from Cassini SAR swath T03). The unnamed 112 km-diameter crater on the left is located at 26°N, 200°W (excerpted from Cassini SAR swath T43).

2.1. ISS images

Imaging of Titan's surface is possible with the Cassini Imaging Science Subsystem (ISS) through an atmospheric window near 0.94 μm. Porco et al. (2005) estimate that ~60–90% of photons at this wavelength are scattered by atmospheric haze at the most ideal geometry of normal incidence and emission, reducing the effective resolution about fivefold. Thus, although pixel scales of a few hundred meters can be attained with ISS, effectively it is difficult to interpret features smaller than ~2 km. Shape from shading is usually not possible because of the effects of scatter. ISS images are consequently limited in their contribution to understanding Titan's geological processes. The significance of resolution limitation is illustrated by the Huygens Probe imaging, which exposed a landscape densely dissected by fluvial erosion, although lower resolution Cassini imaging and radar have not revealed fluvial features at this location (Rodriguez et al., 2006; Soderblom et al., 2007a; Keller et al., 2008).

2.2. VIMS images

The Visual and Infrared Mapping Spectrometer (VIMS) aboard *Cassini*, which observes across the 0.35–5.2 μm wavelength range (with 352 channels), has been used to search for and evaluate geological processes on Titan, including putative cryovolcanic features (e.g., Sotin et al., 2005; Nelson et al., 2009a,b; Soderblom et al., 2009). To its advantage, VIMS can observe the surface through any of eight atmospheric windows, including those at wavelengths near 2.0 and 5.0 μm, which, in principle, permits viewing the surface without significant spatial-resolution-degrading atmospheric scatter. Soderblom et al. (2009) estimate that in the most ideal case of normal incidence and emission, ~44% of the light is scattered at 2.0 μm, while just 10% is scattered at 5.0 μm.

Titan's thick atmosphere restricts Cassini to a closest approach distance of no less than about 900 km from the surface. VIMS imaging of surface features is limited by the instrument's relatively coarse spatial resolution of (at best) 0.25 × 0.5 mrad on a 64 × 64 pixel detector. This translates into VIMS resolutions of ~1 km/pixel at closest approach to Titan. For example, the image of Tortola Facula (see Fig. 4 left) with a resolution of ~1.8 km/pixel is near the limit of the instrument's spatial resolution capability.

2.3. SAR images

There is an extensive literature on interpreting radar data of planetary surfaces, and the difficulties and benefits involved (e.g.,

Ford et al., 1989, 1993 and references with in). Synthetic Aperture Radar (SAR) images, relative to images taken from reflected (or emitted) light, typically exhibit a narrower dynamic range of useful gray scales (and therefore limited contrast), as well as artifacts (e.g., topographic layover, volume scattering, and speckle noise) and ambiguity as to whether return signal strength is due to the scattering properties of the surface or the angle of the slope relative to viewing geometry of the antenna (Elachi, 1988; Ford et al., 1989; Farr, 1993). These are the restrictions that affect the morphological interpretability of Cassini SAR images of Titan's surface.

Cassini's Titan Radar Mapper generates SAR images of Titan with pixel sizes as small as 350 m, but more typically nearer to 1 km/pixel (Elachi et al., 2004). The combination of low resolution and limited grayscale dynamic range means that most landforms on Titan (with the exception of linear features) would need to be ~1 km, and more typically several kilometers across to be identifiable.

Cassini SAR images are acquired at a relatively small incidence angle (usually less than 30°), because of the limited closest approach distance of Cassini from Titan's surface. The effect of small incidence angles is to preferentially accentuate subtle relief, but with the unfortunate effect of enhancing distortion of high-relief features (e.g., Farr, 1993). Where stereo SAR coverage exists, it has been possible to resolve most topographic ambiguities (Kirk et al., 2009). While total Cassini SAR image coverage at nominal mission end is 20%, the stereo coverage at the end of the nominal mission is less than 1% of Titan's surface. The Cassini SAR can be used to generate topographic profiles along two-dimensional transects, which have proven useful in specific instances (Stiles et al., 2009).

Given the limitations in morphological interpretability and coverage of the Cassini SAR images, and the potential influence of erosive exogenic processes on Titan (see Section 3), it is easy to understand why unambiguous identification of Titan's landform morphology—and thus the relative significance of its geological processes—has been challenging.

3. Exogenic processes on Titan

The Cassini Orbiter and the Huygens Probe reveal an Earth-like landscape of fluvial valleys, channels, and lakes interspersed with impact craters and extensive dune fields (e.g. Elachi et al., 2005; Keller et al., 2008). Fluvial and lacustrine processes, aeolian processes, and impact cratering are all exogenic processes, where the energy for surface modification is supplied external to the surface. While simulations of exogenic processes relevant to Titan's surface environment are beyond the preview of this report, such studies are being performed (e.g., Burr et al., 2008; Sklar et al., 2008; Moore et al., 2010). As briefly summarized below, evidence for their action at Titan is very strong. This is in contrast to the existing morphological evidence for cryovolcanism, as we will discuss in Section 5.

3.1. Fluvial and lacustrine processes

Strong argument for fluvial and lacustrine erosion and deposition on Titan has primarily involved landform identification and interpretation in Cassini SAR (Fig. 1) and VIMS images (Stofan et al., 2006; Barnes et al., 2007; Soderblom et al., 2007a; Jaumann et al., 2008; Lorenz et al., 2008); images from the Huygens probe (Soderblom et al., 2007b; Keller et al., 2008); and theoretical scaling of fluvial processes to account for the different gravity, temperature, fluid and material properties of Titan relative to Earth (Ori et al., 1998; Collins, 2005; Parker, 2005; Burr et al., 2006; Perron et al., 2006). Evidence for fluvial processes includes integrated dendritic systems, always originating with diminutive presentation in regions of high topography and becoming more prominent as branches converge down-gradient, where topographic information can be derived or inferred. Where resolution permits, the dendritic systems are seen to be composed of valleys, which in some cases exhibit central channels.

The occurrence of fluvial valley networks is consistent with Titan's methane-rich atmosphere being capable of producing high-intensity convective liquid precipitation events (Lorenz, 2005; Lorenz et al., 2005; Hueso and Sanchez-Lavega, 2006; Perron et al., 2006; Lunine and Atreya, 2008; Turtle et al., 2009; Schaller et al., 2009). The narrow, elongated fluvial depressions on Titan are commonly termed "channels" (e.g., Barnes et al., 2007; Lorenz et al., 2008); however, most are probably more precisely termed valleys (a category that includes surrounding slopes) or floodplains (which are typically not fully occupied by flood flows, i.e. the fluvial discharges produced during a flood). It has been proposed that high-volume discharge floods may have affected broader regions of

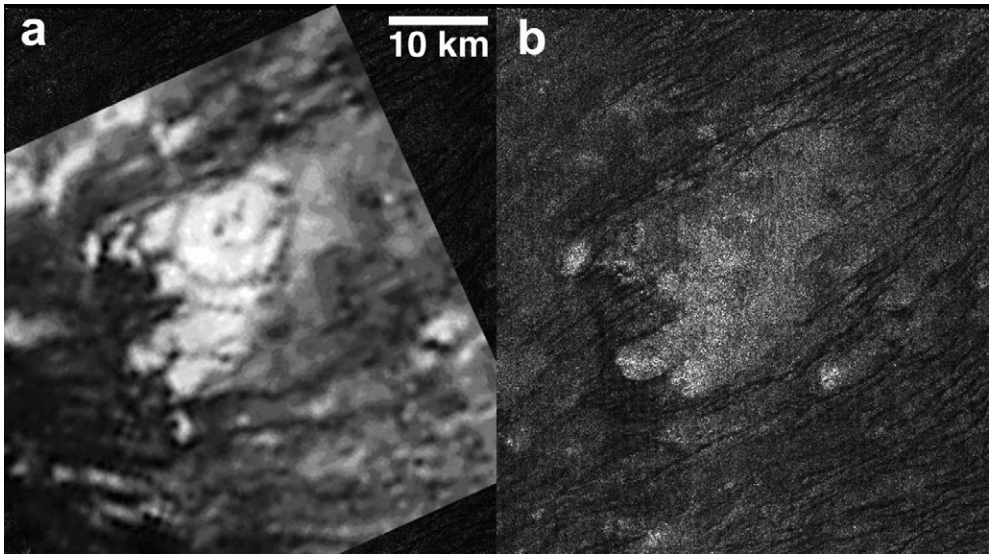

Fig. 4. Tortola Facula (9°N, 143°W), was interpreted as a cryovolcano (Sotin et al., 2005), based on VIMS data (left) collected near the beginning of the Cassini orbital tour (26 October 2004). The nominal resolution is 2 km/pixel. Subsequent SAR imaging (right, excerpted from Cassini radar swath T43) indicates that this feature is a non-descript mountain, such as are commonly found in this region of Titan (see Fig. 2). SAR image nominal resolution is 300 m/pixel.

the satellite (Soderblom et al., 2007b) and potentially could be an important erosional process on Titan, as they have been on Mars (e.g., Robinson and Tanaka, 1990; Craddock and Howard, 2002).

Imaging of Titan's polar regions has revealed landform suites with collective components that are strongly consistent with lacustrine origin (Stofan et al., 2007; Brown et al., 2008; Hayes et al., 2008a; Turtle et al., 2009). Inferred changes in the outlines of some polar Titan lakes suggest ongoing lacustrine activity (e.g., Turtle et al., 2009; Hayes et al., 2009; Wall et al., 2010). Many of these lakes appear to occupy steep-walled depressions that apparently reflect lacustrine shore processes (Mitri et al., 2007; Stofan et al., 2007; Brown et al., 2008; Hayes et al., 2008a), while other lakes appear to have resulted from relatively recent deep immersion of fluvially eroded topography with no obvious shoreline modification by lacustrine processes. These characteristics are diagnostic of lacustrine morphologies and processes. Moreover, convincing evidence that some contain fluids at present comes from IR spectra (Brown et al., 2008) and the definitive observation of glint off of one northern lake (Stefan et al., 2010).

3.2. Aeolian processes

Cassini radar imaging reveals sub-parallel dark striations (Fig. 2) that commonly deflect around topographic obstacles, with morphologies and characteristics that are diagnostic of longitudinal (seif) dunes (Lorenz et al., 2006). These radar-dark features are observed to cross huge tracts of the equatorial surface. They typically overlie brighter materials, which are sometimes revealed in interdune materials. Their deflection directions, *Y*-junctions, and asymmetric streamline pattern all suggest generally eastward transport direction for aeolian-saltated grains (Lorenz et al., 2006; Radebaugh et al., 2007a,b; Lorenz and Radebaugh, 2009). The nature of the aeolian sediment is uncertain, but may consist of organic solids (Soderblom et al., 2007a), which are potentially cohesive (Rubin and Hesp, 2009). No definitive evidence for aeolian erosion of obstacles has been detected, perhaps because of the limitations in available image resolution and spatial coverage.

3.3. Impact cratering

Wood et al. (2010) describe the nature of Titan's impact craters (Fig. 3) and possible modification processes. In the 22% of Titan that has been thus far imaged with radar as of this writing, Titan is reported to possess 7 certain impact craters. Their morphological characteristics such as raised rims, central peaks, ejecta deposits, and inward-facing scarps argue convincingly that these craters are of impact origin. An additional 44 features are more tentatively identified as impact craters that are more degraded, but their is necessarily uncertain because they do not show multiple diagnostic morphologies distinctive of impact craters (Wood et al., 2010).

The certain impact craters include the central peak craters Ksa, Selk, and Afekan (diameters of 30 km, 80 km, and 115 km, respectively); an unnamed 139 km crater with a probable central peak; and Menrva, a 445 km peak-ring basin. The impact crater Sinlap (79 km diameter) appears to be flat-floored in radar images. The majority of craters have dark floors, and all are modified to various degrees. Eastern Xanadu shows by far the greatest density of putative craters, most apparently eroded (Radebaugh et al., 2010). Many craters here and elsewhere are encroached upon by dunes and valleys, indicating that aeolian and fluvial processes have modified the cratered landscape. The nature of the smooth dark material within craters may be wind-carried dust, saltated "sand," or precipitated hydrocarbons. Wood et al. (2010) also considered eruption of icy lava in crater floors as a possible mechanism for these deposits. Titan shows no evidence for palimpsests or central dome craters, in contrast to similarly sized impact features on Ganymede and Callisto, two bodies of similar size, surface gravity, and crustal composition to Titan (see Section 6.1).

The small number of certain identified impact craters combines with the uncertainty in impactor flux to permit an uncertainty in the surface age from as little as 100–500 Myr to as great as 1–3.5 Gyr, as inferred by modeled cratering rates (Artemieva and Lunine, 2005; Korycansky and Zahnle, 2005; Jaumann and Neukum, 2009). Jaumann and Neukum (2009) note that when putative impacts are included, the shape of the size–frequency distribution for large (>80 km) craters is similar to that of Iapetus but depleted by an order of magnitude. They argue that smaller craters are much more depleted, and the size–frequency curve for Titan is shallower than expected for atmospheric shielding alone, such that other processes (exogenic and/or endogenic) have played a major role in burying or destroying small craters.

4. Cautions from other worlds

The experience from past exploration of the solid planetary bodies provides a critical framework in which to consider exploration of a previously unscrutinized world such as Titan. Here we discuss selected lessons from the initial explorations of other worlds regarding the limitations of image spatial coverage and resolution, especially as pertinent to the search for volcanic and cryovolcanic landforms and deposits. These lessons warrant prudence in interpretation of (cryo)volcanism from modest resolution images.

4.1. The terrestrial planets

Analysis and landform interpretation during exploration of the Moon, Mars, and Mercury encountered many of the limitations now presented to Titan investigations. There are the obvious conceptual limitations when grappling with unfamiliar landscapes, because of processes, geological materials, and process dominance and rates that are very different than those previously considered. Early explorations were further exacerbated by limitations in resolution and coverage.

4.1.1. Mariner 6 and 7 at Mars

With its mix of exogenic processes (impact cratering, and fluvial and aeolian processes), and endogenic processes (volcanism and tectonism), Mars makes an interesting comparison to Titan. A good example of the effects of limitations in both resolution and coverage can be gleaned from the 1969 duo flybys of Mars by Mariner 6 and 7 (Fig. 5). Mariners 6 and 7 collectively imaged about 20% of the martian surface at resolutions of ~2 km/pixel or better (with a few narrow angle images with ostensible resolutions of ~100 m/pixel covering less than 1% of the planet), analogous to Cassini radar coverage of Titan. The fine detail discrimination capability (i.e., modulation transfer function and dynamic range) of the camera imaging systems of 1969 were substantially inferior to visible light cameras of today, but are similar to the SAR images of Titan from Cassini. Our knowledge of Mars geology in 1969, was in some respects, comparable to our knowledge of Titan geology prior to Cassini's arrival; therefore, the lessons of early Mars exploration are pertinent.

Much of the Mariner 6 and 7 geological analysis was performed under the careful eye of R.P. Sharp (Leighton et al., 1969a–c; Sharp et al., 1971a,b; Murray et al., 1971; Cutts et al., 1971), a geomorphologist renowned for his meticulous terrestrial work before becoming involved in planetary studies. Among the landforms seen in some of these images were sinuous troughs, which Murray et al. (1971) noted in passing but declined to speculate as to their origin. In fact, the image analysis team did not spend notable time informally speculating even among themselves as to sinuous trough

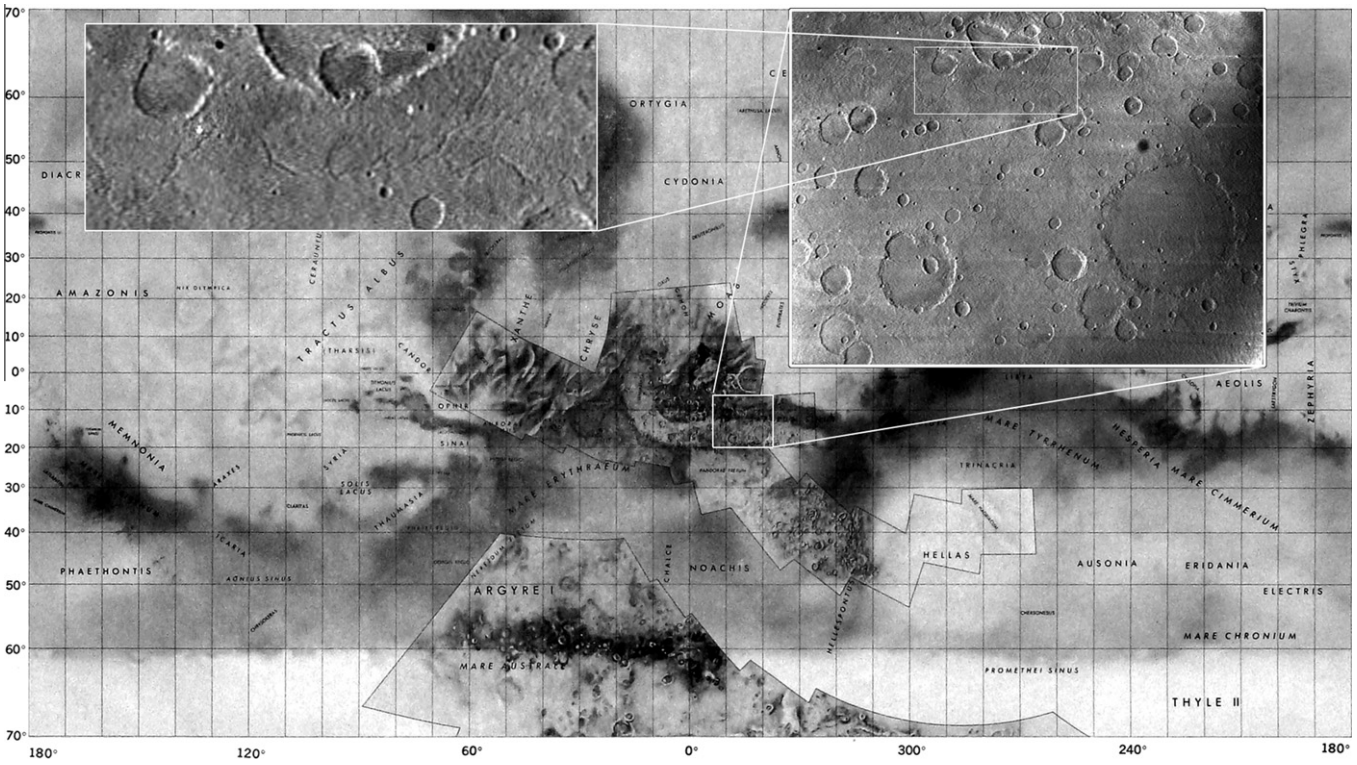

Fig. 5. Mercator map of Mariner 6 and 7 coverage of Mars. Both spacecraft flew past Mars in 1969 producing image coverage of ~20% of the planet at ~2 km/pixel. Much of the rest of Mars was seen at substantially lower resolution. The 1969 Mariner coverage is roughly comparable in areal coverage and resolution to surface imaging of Titan from both the RADAR SAR and the ISS at the end of the Cassini nominal mission. The insets show a single Mariner 6 image (6N21, full frame on right, full resolution enlargement on left). In the upper left inset, the "sinuous trough" subsequently named Evros Vallis is clearly seen. Given the limitations of the data and knowledge of Mars, the Mariner 1969 image team prudently described the feature without attributing it to a geological process. (Mariner 6 and 7 map courtesy L.A. Soderblom, USGS.)

origin (L.A. Soderblom and J.A. Cutts, personal communications). Today we can identify the largest and most conspicuous sinuous trough in the Mariner 6 images as Evros Vallis, which is widely interpreted to have formed by running water (e.g., Howard et al., 2005). In retrospect, it is understandable why the Mariner camera geologic group did not venture past merely describing these features: The best Mariner 6 image of Evros Valles shows very little tributary branching or any other unambiguous features specifically associated with fluvial activity. Moreover, the contemporaneous post-Apollo-landing analysis of much higher quality images of the Moon concluded that the sinuous troughs seen there were volcanic (e.g., Greeley, 1971). It is especially interesting that planetary geologists did not speculate about water-formed features on Mars at that moment, given political stress on the Mars program as it sought continued public funding for the "Mariner 1971" and "Viking 1973" projects (e.g., Ezell and Ezell, 1984, pp. 175–192; Chaikin, 2008, pp. 55–57).

The Mariner 6 and 7 camera team noted that their images did not show low-lying lava-filled basins (as known on the Moon), or any other features which they might have taken as definitive evidence of volcanism. (The 1969 Mariners did not image the martian northern hemisphere sufficiently to see the global dichotomy that *is* there.) On the other hand, they did observe that cratered terrain had been degraded by some process or processes, and an intercrater plains unit was present that was unlike the landscape of the lunar highlands (Murray et al., 1971). These deviations from the lunar landscape were attributed to some unidentified process(es) involving erosion and lateral transport of material. A notable miscall by the team was identification of the ~500 km-diameter bright annulus with a bright central dot in the Nix Olympica region as an impact crater (Leighton et al., 1969a). Today we know this feature as the enormous shield volcano Olympus Mons. Given what the 1969 Mariner camera team could discern and conceptualize of Mars to that date, this was a reasonable and conservative assumption.

In light of subsequent missions, shortcomings of Mariner 6 and 7 images were that their resolutions were insufficient to recognize landforms that are unambiguously diagnostic of high science interest processes (fluvial and volcanic). Moreover, limited noncontiguous coverage did not permit enough examples of definitively interpretable features. Finally, the 1969 state-of-knowledge of Mars may have played a role in the perceptions of the image analysts. These lessons should be borne in mind as the *Cassini* Titan data are analyzed.

4.1.2. The lunar Cayley Plains

Around the same time as the Mariner 1969 flybys, the lunar mapping effort, much of it initially based on Earth-based telescopic observations [see Wilhelms (1993) for historical commentary], was being synthesized into a map of the Moon's near side. Wilhelms (1970) summarized the stratigraphic argument that the smooth light-toned plains unit known as the Cayley Formation, which locally covers the floors and seemingly embays the walls of craters such as Ptolemaeus (Fig. 6a), was of volcanic origin. Although earlier maps suggested that this material might be part of the Fra Mauro Formation, which is interpreted as ejecta from the Imbrium impact, consensus was reached that the Cayley Formation was composed of volcanogenic lavas or tuffs; the relatively high albedo and lack of volcanic landforms were considered to be the result of different composition or greater age than the basaltic mare materials (Wilhelms, 1970, 1976). The outcrops of Cayley material in widely separated "pools" were attributed to discrete volcanic sources. The lack of flow fronts and wrinkle ridges on these units was thought to indicate the materials consisted of tephra.

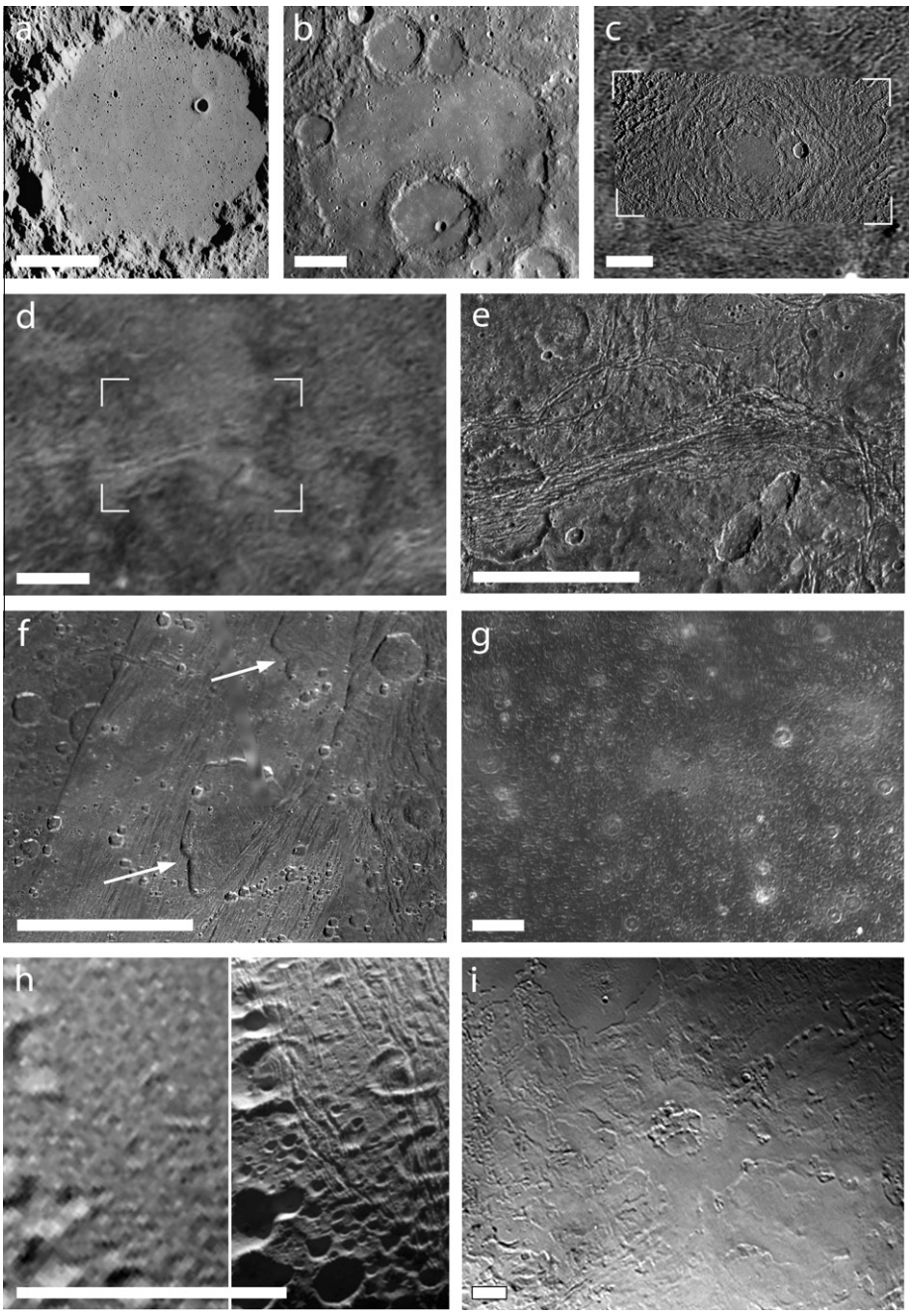

Fig. 6. The search for (cryo)volcanism on the terrestrial planets and icy satellites provides lessons and cautions for the search for cryovolcanism on Titan. Each scale bar is 50 km in length. (a) Light plains materials of the lunar Cayley Formation fill Ptolemaeus crater and other neighboring low-lying highlands regions on the Moon (Apollo Image AS16-M-0990, NASA/JSC/Arizona State University). The smooth materials were at the forefront of the search for highlands volcanism, but instead Apollo 16 samples showed that the Cayley Formation consists of impact breccias associated with basin-forming impacts. (b) MESSENGER images of Mercury support the hypothesis that smooth plains are volcanic in origin (MESSENGER MDIS NAC image EN0108827047M, and PIA10384), based on superposition relationships (here because the smooth material in the large crater embays the ejecta of superposed craters) and an abundance of distinctive volcanic landforms (Head et al., 2008). (c) Like other low-relief palimpsests on Ganymede, the bright circular patch that defines Buto Facula was suggested to be possibly cryovolcanic, based on Voyager images (background Voyager 2 image is ~1.2 km/pixel). Galileo images superimposed within the tick marks (190 m/pixel, Galileo observation G8GSBUTOFC01, and PIA01659) demonstrate that the bright material is impact ejecta, which has excavated brighter subsurface material (Jones et al., 2003). (d) Ganymede's dark terrain exhibits bright patches associated with tectonic furrows, which had been inferred as possibly cryovolcanic in origin (Murchie et al., 1990), as seen in Voyager 1 images at ~1.2 km/pixel. (e) Galileo images at 180 m/pixel (Galileo observation G7GSNICHOL01, showing the area within the tick marks of [d]) illustrate that brightening is the due to a combination of tectonism, impacts, and mass wasting (Prockter et al., 2000), with no indication of associated cryovolcanism. (f) Scalloped depressions (arrows) in Ganymede's bright terrain (43 m/pixel Galileo observation 28GSCALDRA01 superimposed on 150 m/pixel observation 28GSCALDRA02), which may be analogous to volcanic calderas, based on their scalloped morphologies and associations with bright smooth material (e.g. Schenk et al., 2001). The boundaries of Ganymede's scalloped depressions are typically concave-inward, with inward-pointed cusps (e.g. at arrow tips), consistent with inward collapse along listric faults, like those at terrestrial calderas. Comparison to nearby impact craters shows distinctive differences in planform morphology. (g) Variegated albedo materials of Callisto's cratered plains as imaged by Voyager 1 at ~1.7 km/pixel. Some bright and smooth patches were previously considered possibly cryovolcanic in origin (Bender et al., 1997), but high-resolution Galileo imaging indicated that these are related to impact ejecta and mass wasting instead (Moore et al., 2004). (h) Voyager 2 imaging of Samarkand Sulci in the north polar region of Enceladus (left) at 1 km/pixel shows partial craters that were cited as evidence for cryovolcanism (e.g. Squyres et al., 1983b). Cassini images of the same region (right) at 176 m/pixel (PIA08409) instead indicate that tectonism has resurfaced this region, without evidence for associated cryovolcanism. (i) The Leviathan Patera region on Triton presents some of the best evidence for cryovolcanism on an icy satellite: smooth deposits and associated irregular pits radiate from a complex scalloped depression. However, the ~1 km/pixel resolution of the Voyager 2 images warrants caution in this interpretation.

Sampling the Cayley Plains was a critical objective that drove the landing site selection process for the Apollo 16 mission. Another driver was the desire to sample materials from the nearby hills of the Descartes Formation, a unit also interpreted to be volcanic. Samples collected by the astronauts from sites of typical occurrence showed Cayley and Descartes materials to be brecciated materials little different than other highlands materials. The Cayley Formation was then deduced to be composed of impact basin ejecta (Wilhelms, 1976; Muehlberger and Ulnch, 1981), likely deposited from the ancient Nectaris impact and later reworked by Imbrium secondary impact events (Spudis, 1984). The lesson of the Cayley Plains experience is that volcanism, in some cases, may be very difficult to remotely distinguish from other processes using geomorphology alone.

4.1.3. The mercurian smooth plains

The Mariner 10 spacecraft had three flyby encounters with the planet Mercury in 1974 and 1975. It contiguously imaged the available illuminated surface (~40% of globe) at ~1 km/pixel and observed a few locations at resolutions as fine as ~100 m/pixel. The Mariner 10 imaging team reported a Moon-like geology, including high-albedo smooth plains that were interpreted as volcanic (Murray et al., 1974, 1975; Strom et al., 1975; Trask and Guest, 1975). With the recent lesson of the Cayley Formation in mind, interpretations of a volcanic origin for smooth plains were questioned, and an origin as impact ejecta was proposed (Wilhelms, 1976; Malin, 1978). The Mariner 10 camera team acknowledged that the smooth plains unit (termed the Intercrater Plains) exhibited no definitive evidence for volcanism, such as flow fronts, vents, or central constructs. Wilhelms (1976) recognized that the arguments of the Mariner 10 camera team were very similar to those advanced for the volcanic origin of the Cayley Formation, so alternative hypotheses needed to be considered. Plains volcanism would have important implications for the evolution of Mercury (and for the other terrestrial planets), and Wilhelms (1976) emphasized the importance of keeping the question of volcanism open.

Subsequently, recalibration and analysis of Mariner 10 camera color data was pursued, indicating compositional differences between the plains materials and the cratered terrains, supporting a volcanic origin for the plains (Robinson and Lucey, 1997). Open questions of mercurian volcanism were part of the justification for the MESSENGER mission (Solomon et al., 2001). Results from the three MESSENGER flybys show confirmatory evidence for volcanic vents and geological associations (Fig. 6b), augmenting the evidence for plains volcanism (Head et al., 2008; Robinson et al., 2008), though not yet settling this question for all "smooth plains" across the planet. For the mercurian plains, high resolution and compositional data acquired by a later mission permitted remote identification of characteristics diagnostic of volcanism.

4.2. The icy satellites

4.2.1. The Galilean satellites

Lessons from exploration of the Galilean satellites can better inform our understanding of Titan. The concept of icy volcanism, or "cryovolcanism," emerged from examinations of icy satellites surfaces as first acquired by the twin Voyager spacecraft in the 1970s and 1980s. The Galileo mission then provided the opportunity to test cryovolcanic hypothesis by means of much higher resolution imaging, commonly ~10s m/pixel (Carr et al., 1995). In most instances, landforms inferred as cryovolcanic in relatively low resolution Voyager images were found to have other explanations when examined with higher resolution Galileo images. This suggests a cautious approach to interpretation of landforms as possibly cryovolcanic on Titan and other icy satellites.

Europa was imaged by the Voyagers at resolutions too coarse (never finer than ~2 km/pixel) to draw definitive conclusions regarding cryovolcanism, but observations of smooth, bright plains were generally inferred to have been produced by cryovolcanic resurfacing (e.g., Squyres et al., 1983a). On the other hand, Lucchita and Soderblom (1982) suggested that vertical replacement of the lithosphere might have played a more important role. Subsequent post-Galileo analysis found that the bright plains are dominated by vertical tectonic and ridging processes (Greeley et al., 2004), with only occasional (~1–10 km-wide) patches of level smooth terrain that embays surrounding terrain and might have formed as a result of the freezing of a watery extrusion (Fagents, 2003). Galileo images did reveal that chaotic terrains have resurfaced significant portions of Europa, potentially by means of ice diapirism (Pappalardo et al., 1998); however, these chaotic regions comprise Europa's dark "mottled terrain," rather than the bright plains that had been commonly inferred as emplaced by cryovolcanic flows. Lessons from Europa urge caution in interpreting a terrain as cryovolcanic based on uniform and smooth appearance at coarse resolution.

The Voyagers imaged Ganymede both more extensively and at significantly higher resolution (portions up to ~500 m/pixel) than Europa. Bright subcircular patches within dark terrain termed "palimpsests" (Fig. 6c) were suggested to be ejecta deposits (e.g. Passey and Shoemaker, 1982) or sites of impact-triggered cryovolcanism (e.g. Thomas and Squyres, 1990). Analyses of higher resolution Galileo images indicate that the bright palimpsest material is brighter impact ejecta excavated from below (Jones et al., 2003; Schenk et al., 2004), rather than cryovolcanic material.

From Voyager images, Ganymede's dark terrain was interpreted as an old, heavily cratered surface buried by overlapping blankets of cryovolcanic material (Fig. 6d), an interpretation supported by inferences of depleted small crater densities, embayment of large craters, and smooth areas associated with furrows (e.g. Murchie et al., 1990). Schenk and Moore (1995) proposed that volcanic activity on Ganymede included extrusion of icy materials into crater floors to form lobate domes and into furrow floors to create smooth dark deposits. But higher resolution Galileo images reveal no unequivocal identification of dark terrain volcanism, such as lobate materials with an identifiable source vent. However, some candidate cryovolcanic units identified at low resolution on the basis of embayment and texture instead seem to have formed as fluidized impact ejecta or from fine-scale tectonism (Fig. 6e). Moreover, smooth dark materials in topographic lows probably accumulated by downslope movement of loose material (Prockter et al., 2000; Pappalardo et al., 2004). While it is possible that evidence for cryovolcanism could potentially exist below the current limits of image resolution or in dark terrain areas not yet imaged, the hypothesis of dark terrain cryovolcanism is not supported by the Galileo imaging data.

The interpretive view of Ganymede's bright grooved terrain that developed from Voyager images held that light-toned cells of proto-grooved terrain were broad graben, cryovolcanically infilled by the extrusion of relatively clean (silicate-poor) liquid water, warm ice, or icy slush which was subsequently stretched and fractured (Shoemaker et al., 1982). Analyses of Galileo data led to substantially revised ideas: direct evidence for bright terrain cryovolcanism is rare, with scalloped depressions associated with some smooth terrains (Fig. 6f) being the best evidence, inferred to be caldera-like features from which smooth cryovolcanic material may have extruded (Schenk et al., 2001; Pappalardo et al., 2004). The dominant post-Galileo conception of Ganymede's bright terrain formation argues that "resurfacing" (i.e., erasure of craters) can be accomplished through pervasive extensional tectonism, while most evidence of associated cryovolcanism, if present, is destroyed by subsequent tectonism (Pappalardo et al., 2004). The

post-Galileo role of cryovolcanism in shaping Ganymede's surface is much reduced relative to what had been initially inferred from lower resolution Voyager images.

There was speculation from Voyager images that some bright and/or smooth patches on Callisto (Fig. 6f) might be cryovolcanic in origin (Melosh, 1982; Bender et al., 1997), making the search for cryovolcanism a priority for Galileo imaging (Carr et al., 1995). Galileo observations revealed an exotic form of widespread erosion, but otherwise found no evidence that cryovolcanism has operated on Callisto's surface (Moore et al., 2004). The bright and dark patches in Voyager images were shown to be bright impact-related materials (palimpsests and other impact ejecta) and smooth dark deposits created by mass wasting. Despite evidence of an internal ocean and differentiation of the outer ice shell (Schubert et al., 2004), the post-Galileo view of Callisto is of an endogenically quiescent world (Moore et al., 2004), yet one that remains fascinating and mysterious (McKinnon, 1997).

4.2.2. The icy middle-sized satellites of Saturn

Cautions regarding the interpretation of cryovolcanism extend to the middle-sized icy satellites of the saturnian system, where Cassini images show that the role of cryovolcanism is significantly more limited than had been thought from low resolution Voyager images, which partially mapped the middle-sized icy satellites of Saturn at ~1-km resolutions and coarser. Voyager images suggested that the satellites' surfaces were dominated by impact craters, but limited tectonic and cryovolcanic activity were also interpreted (see reviews by Squyres and Croft (1986), Johnson (2005); and Collins et al. (2009)).

A cryovolcanic resurfacing model was applied to the "smooth plains" of Enceladus (e.g., Squyres et al., 1983b) based on Voyager data (Fig. 6h, left). However, when viewed at high resolution by Cassini, Enceladus is instead heavily tectonized at a small scale (Fig. 6h, right), and evidence for "cryovolcanism" on Enceladus is in the form of venting of H_2O jets, rather than water-rich slurries (e.g. Spencer et al., 2009). Voyager images revealed "wispy" terrains at Dione and Rhea, which were speculated to result from pyroclastic cryovolcanism (Stevenson, 1982). Cassini's imaging resolution has revealed that the bright scarp faces of closely-spaced small-scale faulting is instead responsible for the wispy appearance (Jaumann et al., 2009b). The variety of endogenic features found on Tethys, Rhea, and Dione do not result in landforms that are conclusively diagnostic of effusive cryovolcanism, but could be explained by tectonic distortion and resurfacing without effusive eruptions. As at the Galilean satellites, the middle-sized saturnian satellites illustrate that cryovolcanism is uncommon and/or elusive.

4.2.3. Triton: evidence for cryovolcanism

Triton, the single large satellite of Neptune, shows strong evidence for cryovolcanism. Triton was imaged regionally by Voyager 2 over the illuminated hemisphere at ~1–3 km/pixel and locally at ~500 m/pixel. These images reveal a young surface with landforms that include candidate flow lobes and (cryo) pyroclastic plains, as well as ridges and troughs that are more likely tectonic (Croft et al., 1995; Collins et al., 2009). The most dramatic evidence for cryovolcanism is at Leviathan Patera (Fig. 6h), which consists of several large nested arcuate scarps surrounded by a smooth mantled terrain that feathers distally from the scarp complex; its characteristics closely resemble those of large caldera-collapse pyroclastic features on Earth and Mars (Croft et al., 1995). Moreover, Triton shows ~100 km-wide (scarp enclosed) smooth plains that have morphologies and textures suggestive of cryovolcanic emplacement (Croft et al., 1995). These features of Triton are considered to be the best evidence for large-scale cryovolcanism on the icy satellites, and are presumably related to the abundance of volatile ices there (Schenk and Moore, 1998; Johnson, 2005).

When weighing the Voyager evidence for cyrovolcanism on Triton, we must keep in mind the significant revisions of cyrovolcanic concepts for the geological histories of the Galilean and middle-sized saturnian satellites following high-resolution imaging of their surfaces by Galileo and Cassini. With rare exception, higher resolution imaging of icy satellites has shown that cryovolcanism is a less common process than previously believed based on lower resolution images, which tend to make landscapes appear artificially smooth. It is also interesting to note that there are no recognized examples of volcanic mountains on any airless icy satellite.

5. Case studies of putative cryovolcanic features on Titan

The lessons of the past outlined in the previous section urge caution in assigning a volcanic origin to landforms on Titan. Trends emerging from these historical investigations strongly indicate that low resolution can result for example in the illusion of smooth textures. Aspects of other processes can mimic volcanic landforms. For instance, mass wasting, fluvial deposition, and impact ejecta can produce flows and flow-like textures. Insufficient resolution to distinguish those aspects of flows, flow textures and associated landforms that are unique to volcanism make recognition of volcanism on other worlds particularly problematic.

Several features observed in Cassini SAR and VIMS images acquired during the Cassini prime and Equinox missions have been identified as cryovolcanic in origin (see summaries by Lopes et al. (2007) and Jaumann et al. (2009a)). Here we consider several case studies based on published interpretations of cryovolcanism on Titan: Tortola Facula, Ganesa Macula, and Hotei Regio, and also additional irregular lobate features. All are found to represent negligible or equivocal evidence for cryovolcanism (in strong contrast to the strong morphological evidence for exogenic landforms and processes, as discussed in Section 3). Instead Titan's landforms are consistent with an endogenically quiescent Titan; we also briefly consider the role of possible tectonic features.

Experience with unambiguous volcanic landforms provides diagnostic criteria for their recognition. Volcanic effusion is primarily an accretionary constructive (positive relief landform building) process, generally with a negligible erosive role. The criteria for volcanic deposits include recognition of flow fronts that are commonly distally distributive, distinctive flow textures that are most often the result of differential shear within the flow during emplacement, identification of source vents with clearly seen topographic components, and embayment and superposition relationships of the flows over pre-existing surfaces as well as small scale morphological features such as tumuli, channels, and pits due to lava tube collapse. Flow deposits themselves are often overlapping as a consequence of successive eruptions. For instance the combination of deposits producing positive relief from overlapping flows could indicate a volcanic origin.

5.1. Tortola facula

VIMS data at ~2 km per pixel, acquired during a Titan pass soon after Saturn orbit insertion in July 2004, show an infrared-bright feature (Fig. 4a) at 9°N, 143°W, sometimes informally referred to as "snail-shaped" (e.g., Lopes et al., 2010) and subsequently named Tortola Facula. Sotin et al. (2005) described this as a bright circular feature about 30 km in diameter, with two elongated wings extending westward. They inferred that Tortola Facula was topographically higher than its surroundings based on its relative reflectance as a function of wavelength. They noted that the center pixel was much darker than its surroundings, and commented that

"it is quite tempting to imagine a caldera-like feature in the centre." Sotin et al. (2005) argued that the feature resembles volcanic edifices with lobate flows, such as those observed on Earth or Venus. Sotin et al. (2005) concluded by interpreting Tortola Facula as a cryovolcanic dome in an area dominated by tectonic extension, and that eruptions from it may release large amounts of methane into Titan's atmosphere.

A 300 m/pixel SAR image of Tortola Facula acquired on the T43 flyby in May 2008 (Hayes et al., 2008b) shows the feature to be a patch of mottled non-descript radar-bright terrain, surrounded by radar-dark dunes that divert around the feature (Fig. 4b). Earlier impressions of concentric ridges and a central caldera are instead found to be the low-resolution effect of a complex interplay of small-scale reflectance and topographic variations. Blocks and patches of radar-bright (commonly hummocky) terrain amidst dune ergs are now known to be common in this region, designated Shangri-la (see Fig. 2). Such patches are generally inferred to be radar-bright mountainous terrain (cf. Radebaugh et al., 2007b). Lopes et al. (2010) explicitly note that Tortola Facula is now among patches of material they classified as the *hummocky and mountainous terrain*, rather than cryovolcanic.

5.2. Ganesa macula

Ganesa Macula (50°N, 85°W; 180 km-diameter) was identified in the first SAR observation of Titan (orbit Ta) in October 2004 (Fig. 7). It was described as a radar-bright border apparently surrounding radar-dark material, with a central bright spot from which at least four sinuous lineaments radiate out to the perimeter (Elachi et al., 2005). Ganesa Macula was interpreted as a volcanic edifice, either a dome or a shield volcano, and radar-bright lobate materials to the east named Leilah Fluctus were considered flows of material that emanated from Ganesa (Elachi et al., 2005; Stofan et al., 2006; Lopes et al., 2007). Lopes et al. (2007) noted the similarity of the radar presentation of Ganesa Macula to Magellan SAR images of "pancake" domes on Venus, which SAR images imply are steep sided and flat topped. Encouraged by this interpretation, follow-on studies reported on modeling of the eruption and rheological characteristics that the formation of such features would indicate (Neish et al., 2006; Fortes et al., 2007; Mitri et al., 2008; Zhong et al., 2009). Ganesa was commonly cited as the archetypal example of cyrovolcanism on Titan.

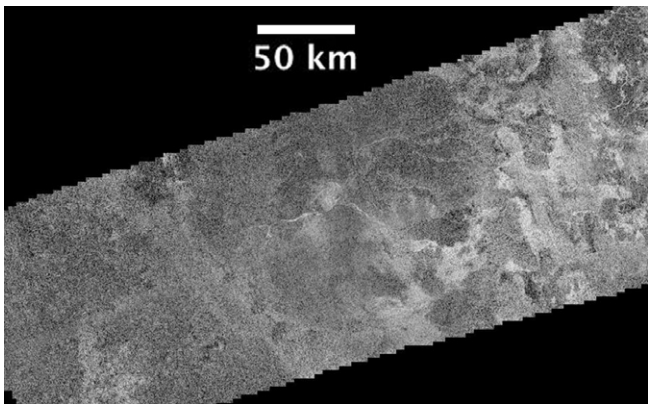

Fig. 7. The circular ~180-km-diameter feature in the center of this image was observed in the first SAR image swath (Ta) acquired by Cassini in 2004 and subsequently named Ganesa Macula (50°N, 85°W). Ganesa Macula was interpreted in a number of studies as a possible cryovolcano. In monoscopic images it resembles in some respects the so-called pancake dome volcanoes on Venus, though the Venusian examples are a factor of several smaller in diameter. Subsequent stereo-derived topographic analysis indicates that Ganesa Macula is not a coherent topographic dome but instead a collection of high and lowlands.

Subsequently in January 2007, an additional SAR pass (T23) was obtained over Ganesa with an opposite-looking viewing geometry. This permitted "radargrammetric" (stereo) analysis of the two overlapping SAR swaths, providing topographic information for Ganesa Macula and its surroundings. Topographic results indicate that for Ganesa Macula itself there is little or no topographic expression of a dome or shield (Kirk et al., 2009). Kirk et al. (2009) note that Ganesa Macula appears to be part of a larger trough system exhibiting modification by erosion or other processes. Rather than being cryovolcanic flows, fans of Leilah Fluctus to the east of Ganesa are likely depositional fans instead, as suggested by Paganelli et al. (2005). With this hindsight, Furfaro et al. (2010), in developing a technique for automated detection of suspected cryovolcanic features in SAR data of Titan, indicate positive test detection of cryovolcanism at Ganesa and to its east with the Ta SAR data alone, and negative detection when including the SAR-derived stereo topographic information. The misidentification of Ganesa Macula as a cryovolcano was due to a lack of topographic information plus low resolution.

5.3. Hotei regio

Another widely reported example of possible volcanic features on Titan is the case of bright and dark features with lobate margins within Hotei Regio (Fig. 8), near the 650-km long semi-circular feature Hotei Arcus. Nelson et al. (2009a,b) report IR-bright features with lobate margins within Hotei Regio, and infer temporal changes in brightness in this vicinity, which they attribute to changes in amounts of ammonia frosts.

Wall et al. (2009) report from two different SAR swaths that there are many light gray features within Hotei Regio, apparently overlaid on a darker substrate, approximately corresponding to the IR-bright region observed by Nelson et al. (2009a,b). The SAR-brighter units show well-defined lobate boundaries, they exhibit generally uniform radar backscatter, and some larger patches appear to consist of overlapping units. Wall et al. (2009) interpret the bright features with lobate margins as multiple, coalescing cryovolcanic lava flows, where the SAR-brighter unit has flowed over the darker substrate. They note that radar images of lava flows on Earth and Venus show similar lobate shape, texture, and brightness. Moreover, high radar backscatter is generally associated with relatively high roughness and hence potentially relative youth on terrestrial flows, given a lack of erosion and infilling.

Kirk et al. (2009) used SAR stereo-derived topographic data to infer that the lobate radar-bright features of Wall et al. (2009) are instead mostly flat and co-level (notably in the mushroom-shaped "lobe" generally used as an example; see Fig. 2, arrow A in Soderblom et al., 2009), representing usually the *lowest* relief in the region of stereo overlap. Rising above these radar bright plains are low undulating hills with darker and mottled radar brightness (Kirk et al., 2009). Soderblom et al. (2009) note that these low undulating hills with dark and mottled radar brightness are anomalously bright in VIMS images. Soderblom et al. (2009) refer to the cryovolcanic interpretation of the materials with lobate boundaries by Wall et al. (2009) to build on the notion of volcanism in this region, further suggesting that two large roughly circular areas seen only in VIMS data might be calderas. Soderblom et al. (2009) also note that south-debouching valleys (discussed next) as well as the materials with lobate boundaries all lie within a regional basin, which they speculate may have originated as a very large impact feature. Finally, these authors argue that cryovolcanism has occurred in the past rather than at present, illustrating that the inferred temporal changes in Hotei Regio of Nelson et al. (2009a,b) are instead probably a combination of resolution and emission angle effects related to atmospheric scattering.

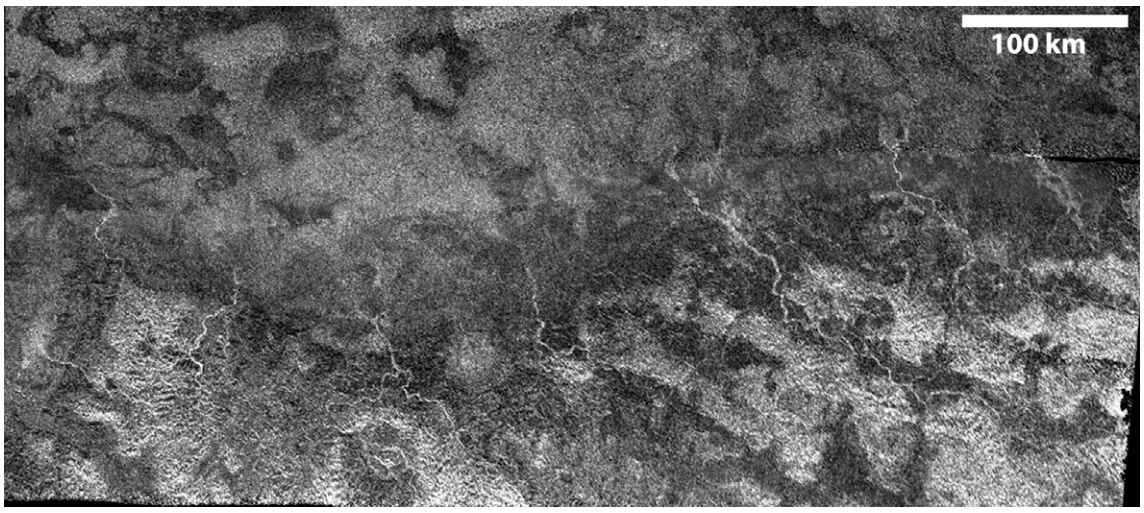

Fig. 8. A region along the northern flank of Hotei Arcus (centered ~30°S, 76°W). The bright surfaces with sinuous (or "lobate") borders along the northern third of the figure have been interpreted in several studies as possible cryolava flows. Subsequent stereo-derived topographic analysis indicates that these bright surfaces are nearly level and the lowest topography in this scene. An alternate explanation is that the bright surfaces are fluvial or lacustrine deposits related to the drainage networks observed along the southern two-thirds of this figure (excerpted from Cassini radar swath T41, north is to the top).

The presence of many radar-bright valleys (probably fluvial), which we interpret as running out onto the radar-bright lobate materials from the highlands to the southeast (Fig. 8), invites an alternate explanation for the bright lobate traces. Soderblom et al. (2009) suggest that the fluvial textures associated with these valleys are limited to small basal "VIMS dark blue units"; however, our examination of the SAR imaging leads us to conclude otherwise. We infer that the bright materials result from fluvial erosion and downcutting of channels, as is commonly observed in sediment-filled valleys on the Earth. Here the radar brightness of the plains unit could be attributed to coarse alluvium, or a desiccation texture, both of which are common on terrestrial playas, and observed in SAR images (for example, of Death Valley, California). The radar-bright alluvium occurs among radar-dark hills we interpret as remnants of older high-standing topography diminished by erosional lowering, rounding, and scarp retreat. Consistent with this, Moore and Howard (2010) suggest that Hotei Regio may be the site of an ancient sea bed (or paleolake clusters), analogous to smaller polar dry lake beds that have been previously inferred (Hayes et al., 2008a). Compared to the cryovolcanic hypothesis, Occam's razor suggests that this fluvial-lacustrine explanation is both simpler and consistent with existing observations, given the strong evidence of widespread fluvial and lacustrine process on Titan.

5.4. Other flow-like features

Many other features on Titan previously have been speculated to be cryovolcanic in origin, based on lobate or irregular morphology (Fig. 9). A "bright lobate unit" in SAR images has been identified and mapped as potentially cryovolcanic, with boundaries that range from distinct to gradational and showing variable brightness across the unit (Elachi et al., 2005, 2006; Stofan et al., 2006; Lopes et al., 2007). In first characterizing such a unit, Elachi et al. (2006) explicitly cite previous identification of Ganesa and Tortola as rationale to infer that cryovolcanism occurs on Titan to form irregular radar-bright features. Current indications that neither Ganesa nor Tortola shows evidence for cryovolcanism weakens the case that other more poorly characterized lobate radar-bright patches are cryovolcanic in origin.

Lopes et al. (2007, 2010) identify several circular depressions in SAR images as "calderas" each associated with an apparent "flow" (Fig. 9). Possible cryovolcanic implications of one such feature (Fig. 9g) are considered by Le Corre et al. (2009), and a similar feature (Fig. 9d) is identified in VIMS and ISS data by Barnes et al. (2006). The limitations of Titan images (Section 2) necessarily make the identification and description of these features somewhat equivocal. A possible explanation for the origin of a circular depression associated with lobate material is the coincidence of an impact crater with fluvially or aeolian eroded and/or deposited radar-bright material. Better understanding of the nature and origin of Titan's putative "caldera-like" features will certainly come from further imaging and mapping of Titan's surface units, modeling of fluvial and aeolian erosion, and modeling of deposition processes.

Taken as a whole, the examples of candidate cryovolcanism on Titan reported so far are necessarily equivocal. Indeed, two of the most widely cited examples of cryovolcanism, Tortola Facula and Ganesa Macula, are now known to be unremarkable, with no apparent evidence of cryovolcanism when viewed at higher resolution (Tortola) or when seen with associated stereo-derived topography (Ganesa). The cryovolcanic interpretation of a third well known example, at Hotei Regio, has been inverted to correspond to updated topographic information, and evidence for temporal change is probably spurious. Instead, fluvial processes can alternately explain the characteristics of Hotei Regio features. Other irregular and lobate features on Titan may similarly have alternative, and simpler, exogenic explanations. The possibility that these features or others on Titan may be cryovolcanic cannot yet be ruled out, but evidence for cryovolcanism is not compelling.

5.5. Tectonism

Identification of tectonic features on Titan is generally less problematic than are the cryovolcanic candidates. Early notions of extensional-tectonic "grooved terrain" inferred from VIMS and SAR images of Titan (Sotin et al., 2005; Elachi et al., 2005) have not proved true, and are probably related to aeolian processes instead. Nonetheless, there is little doubt that SAR images show linear ridges and other structural features (Radebaugh et al., 2007b; Paganelli et al., 2010). Paganelli et al. (2010) note that Titan SAR images show subtle but distinctive structural geological features, including lineaments, ridges, and linear terrain boundaries, and potentially structurally controlled valleys and lakes.

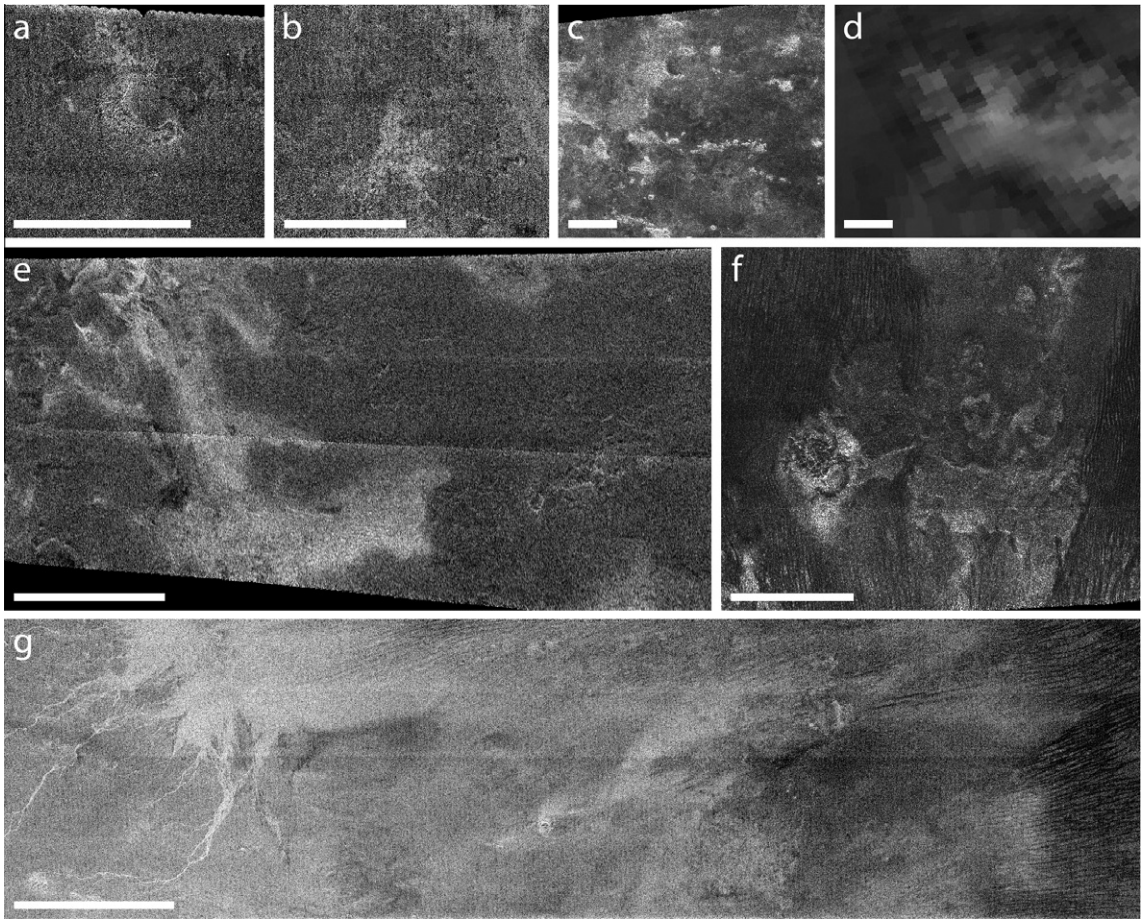

Fig. 9. Examples of features that have been interpreted previously as cryovolcanic in origin may have alternative interpretations, but confident interpretation is hampered by poor resolution and incomplete understanding of the geological processes that might shape Titan. Each scale bar is 100 km in length. (a) An oblong crater and bright arcuate region, previously interpreted as a caldera and associated flow (from Ta SAR). This could be the coincidental occurrence of an impact crater and irregularly mottled materials. (b) A bright amoeboid shaped feature, which may have a small crater at its center, has been previously interpreted as a cryovolcanic caldera and flow (from Ta SAR). Mobilized impact ejecta seems a viable alternative hypothesis. (c) A semi-circular feature amidst radar-bright and radar-dark materials, previously interpreted as a cryovolcanic caldera and flow (from T8 SAR). This could possibly be an impact crater with a rim that has been partially eroded. (d) A combination of images of western Tui Regio (from VIMS Ta at 40 km/pixel and VIMS Tb at 20 km/pixel), bright at 2.0 and 5.0 μm, has been previously interpreted as showing a series of cryovolcanic flows (from Barnes et al. (2006)). ISS imaging suggests a crater at the juncture of the bright features. It seems plausible that the lobes might represent crater ejecta, or some other unknown bright materials. (e) At left are radar-bright materials named Winia Fluctus, previously interpreted as cryovolcanic flow lobes (from Ta SAR); however, dunes cross portions of Winia Fluctus (Lopes et al., 2010), calling into question the interpretation as high topography. It seems plausible that mass wasting and/or fluvial processes have shaped this surface. At right is a crater and nearby mottled materials, previously interpreted as a cryovolcanic caldera and associated flows. Alternatively, this could be a coincidence of an impact crater and an irregular surface. (f) A depression and materials near Sotra Facula (from T25 SAR) has been suggested as a cryovolcano and associated flows (Kirk et al., 2010). Interpretation of these materials should also consider other mechanisms to create depressions and (the currently unexplained origin of) other scalloped and rounded features in the region, which plausibly could involve exogenic processes. (g) Across the center of this scene (from T3 SAR) are features previously interpreted as a cryovolcanic source region and associated flow; its composition has been analyzed in a cryovolcanic context by Le Corre et al. (2009) using VIMS data. Sufficient context is provided here to show that other nearby radar-bright materials are associated with fluvial valleys (Elivagar Flumina, at left), and that the boundaries of the putative flow are aligned similarly to nearby aeolian features (at right and at top). These associations suggest that the central materials may have been deposited and/or subsequently shaped by fluvial and/or aeolian processes.

Radebaugh et al. (2007b) note that large-scale ridges apparently have bedrock central cores, and commonly exhibit downslope fluting surrounded by radar-diffuse peripheries, interpreted as material eroded off the mountain-like ridges by fluvial and other mass wasting processes. In fact, it is plausible Titan's radar-bright mountains may be the result of global contraction, which may build mountains as folded or thrusted blocks (Mitri et al., 2010a). Radebaugh et al. (2007b) examine several possible formation mechanisms for mountains, including crustal contraction and upthrusting of blocks, extensional tectonism with formation of horst-and-graben, deposition as impact ejecta blocks, or dissection and erosion of pre-existing material. They conclude that all the above processes may be at work, given the diversity of geology evident across Titan's surface. Tracts of rugged highlands in Titan's Xanadu province exhibit arcuate and parallel structural lineation that is potential evidence for extensional and contractional tectonism (Radebaugh et al., 2010). Arcuate and parallel structural textures on Titan, as well as well-separated parallel ridges observed elsewhere in the Xanadu region have also been interpreted as expressions of tectonism (Mitri et al., 2010a).

On the terrestrial planets or outer planet satellites, tectonic features can arise as the result of internal heat transport processes, such as solid-state convection. However, outer planet satellite tectonic features do not necessarily indicate a geologically active interior. Instead, changes in a satellite's figure due to internal cooling, orbital evolution, or rotational state can give rise to tectonics-inducing stress. Cooling and freezing of an internal ammonia–water ocean is modeled as giving rise to global contraction of Titan, which may create mountains (Mitri et al., 2010a). Global tectonism might also be induced by tidal flexing due to orbital eccentricity,

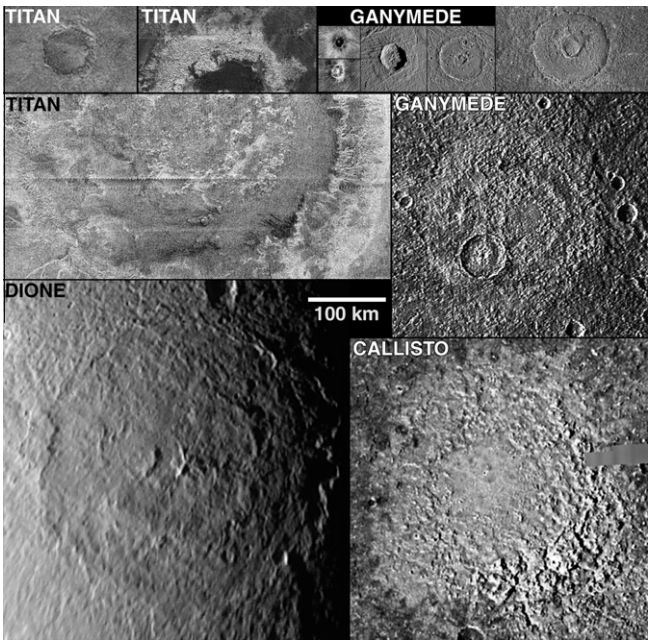

Fig. 10. A montage of impact features on Titan (upper left panels) compared with those of Ganymede and Callisto (right-hand panels) and Evandor basin on Dione (lower left panel), all shown to a common scale. Note that the largest impact craters on Titan do not resemble similar-sized impact features on Ganymede or Callisto. The largest known Titan impact feature (Menrva, middle left) instead shows morphological similarity to similar-sized impact features on other saturnian satellites, such as Evandor on Dione. (All non-Titan images are courtesy Paul Schenk.)

orbital recession or progression, or nonsynchronous rotation (Paganelli et al., 2010). On Callisto, which shows little evidence of endogenic activity, parallel straight to arcuate ridges and scarps, typically similar in scale to those on Titan, owe their origin to multi-ring basin-forming impacts (notably Valhalla and Asgard). Global and regional scale mapping of tectonic elements along with geophysical modeling is necessary to understand the driving processes of Titan's tectonic structures, and whether they provide evidence for endogenic geological activity at Titan.

6. Geophysical consistency with a quiescent interior

The chemistry of Titan's atmosphere is commonly cited as a reason to suspect endogenic activity at Titan, as discussed in Section 7. But first, here we examine several geophysical arguments that are consistent with a cool and quiescent interior at Titan, which would be consistent with a lack of cryovolcanic features on the satellite.

6.1. Impact craters

The morphologies of large craters of Titan diverge significantly from similar-sized impact features on the Galilean satellites (see Section 3.3), despite the similar bulk compositions and gravitational accelerations of these satellites (Fig. 10). Although we do not attempt a thorough and quantitative analysis here, we point to first-order issues that should be further investigated.

Impact craters on Ganymede and Callisto in the range ~35–60 km diameter exhibit central pits, while and craters ~60–175 km diameter exhibit central domes (Schenk et al., 2004). These have been related to the presence of warm, mobile material in the shallow subsurface at the time of impact (Schenk et al., 2004; Senft and Stewart, in preparation). With the caveat that many of Titan's craters are highly eroded, those recognizable craters in this size range do not show such morphologies. This suggests that its icy lithosphere may not have been warm when its similarly sized impact craters formed, or any such morphological indicators on Titan have been subsequently erased as through erosion.

Impact features larger than ~200 km in diameter on Ganymede and Callisto are typically palimpsests with little vertical relief (typically <1 km overall), and can have central regions that are higher than the surrounding terrain, and thus in the strict geometric sense, are not "craters." In contrast, the largest impact feature thus far observed on Titan (445 km-diameter Menrva), though eroded, resembles the peak-ring basins seen elsewhere in the Saturn system, such as Evander on Dione (Fig. 10) or Odysseus on Tethys. In addition to the striking difference in appearance between Menrva and similar-sized impact features on Ganymede and Callisto, regionally the outer floor (the portion between the rim and the peak rim) of Menrva lies ~500 m below the rim, as shown in Fig. 10 of Stiles et al. (2009) (Wood et al., 2010), which is much more relief than is typical of Galilean impact features of similar size (e.g., Schenk et al., 2004). The regional relief within Menrva is all the more remarkable because the outer floor of Menrva exhibits strong evidence of substantial fluvial sediment fill (Wood et al., 2010), and because its original topography has been somewhat eroded. The fact that Titan retains a large deep impact basin with morphologies analogous to similar sized basins on the other saturnian satellites, but very different from the palimpsest-like features of Ganymede and Callisto, suggests that the strength of the icy lithosphere at the time of, and following, Menrva's formation was significantly greater than at Ganymede and Callisto at the time that their palimpsest impacts formed, and closer to that of Dione or Tethys. The apparently stiff icy lithosphere at Titan is consistent with a relatively low heat flux during the presumably broad period of geological time that its impact craters represent.

6.2. Incomplete differentiation

Titan's axial moment of inertia has been derived from Cassini Doppler tracking of the Cassini spacecraft, indicating an interior state intermediate between partially differentiated Callisto and fully differentiated Ganymede (Iess et al., 2010). Interior models consistent with these data suggest that Titan is partially differentiated with an internal mixed ice–rock layer, and/or it contains a hydrated rock core (Iess et al., 2010; Mitri et al., 2010b).

Formation models suggest that Titan must have accreted slowly in order to remain cool and incompletely differentiated (Mitri et al., 2009, 2010b; Mosqueira and Estrada, 2009; Sotin et al., 2009; Barr et al., 2010; Iess et al., 2010). Barr et al. (2010) suggest that Titan could have avoided subsequent full differentiation by large impacts during the late heavy bombardment, instead remaining partially differentiated, with a clean outer ice shell and a central rocky core.

The likelihood that Titan is partially differentiated changes the paradigm in our thinking about the satellite's heat budget and history. It seems unlikely that Titan is or has ever been a very warm and active satellite in the vein of Europa or Ganymede, or that tidal heating is significant within. This tempers expectations regarding cryovolcanism, given that any cryovolcanism is expected to be tied to interior heat loss and evolution. Titan may be more akin to Callisto, with a heat budget dominated by radiogenic heating and loss, as discussed next.

6.3. Convection, tidal heating, and shape

Because convection and any cryovolcanism would be plausibly linked (e.g. Tobie et al., 2006), it is valuable to consider whether Titan's outer ice shell might be convecting. It has been argued that Titan may have experienced convection in the past, and potentially

through the present day (Grasset et al., 2000; Sohl et al., 2003; Tobie et al., 2005, 2006; McKinnon, 2006; Grindrod et al., 2008; Mitri et al., 2008, 2010a; Sotin et al., 2009). In fact, Titan is required to convect during its thermal evolution in order to lose its radiogenic heat while remaining incompletely differentiated (e.g. Barr et al., 2010). Tobie et al. (2006) devise a scenario where Titan enters a convective regime relatively late in its history, potentially triggering cryovolcanism in methane clathrate ice. Mitri et al. (2010a) consider a scenario in which Titan's outer ice shell has cooled to the point where convection halted in recent geological time. Whether Titan's thick ice shell convects today depends on the heat flux from below and the ice shell rheology. The possible presence of clathrate within Titan's ice shell complicates the issue, but the rheology probably principally depends on the temperature of Titan's probable internal ocean, which is in turn controlled by the ammonia concentration (Sohl et al., 2003; Nimmo and Bills, 2010). If significant tidal heating occurs, convection, tidal heating, and interior evolution are inherently linked, as the amount of tidal heating in turn depends upon whether convection warms the ice shell, increasing its dissipation (Sohl et al., 1995; Sotin et al., 2009).

Zebker et al. (2009) infer from radar altimetry data that Titan's global shape is lower at its poles than would be expected from tidal and rotational distortions, given Titan's present rotation rate and distance from Saturn. They hypothesize that Titan's shape was frozen in place when Titan was closer to Saturn than it is today. In contrast, Iess et al. (2010) conclude that Titan's gravity field is inconsistent with this interpretation, finding instead that Titan is consistent with hydrostatic equilibrium with its present rotational and tidal distortions. Instead, the gravity field implies that Titan's icy shell is warm enough today to permit compensation of its surface topography.

Nimmo and Bills (2010) find that Titan's long-wavelength shape (as defined by Zebker et al. (2009)) is consistent with a relatively cool and conductive ice shell, which experiences minor tidal heating and nearly chondritic heat flux, generating topography as a result of lateral variations in ice shell thickness. They find that Titan's present shape is *inconsistent* with a relatively warm and convective ice shell that experiences significant tidal heating, where topography would vary in response to lateral differences in heat production.

Together the results of Iess et al. (2010) and those of Nimmo and Bills (2010) suggest that Titan's global shape and gravity indicate an outer ice shell that is warm enough to be hydrostatic and dissipate a small amount of tidal heat, but potentially too cool to convect today. Such is consistent with conduction and sluggish flow of ice, resulting from radiogenic heating and only minor tidal dissipation.

6.4. Orbital evolution

Today Titan possesses a finite orbital eccentricity of 0.029, which is difficult to reconcile with a highly dissipative Titan, as its primordial eccentricity is expected to circularize over the age of the Solar System (e.g., Sohl et al., 1995). Previous arguments have focused chiefly on whether Titan's present eccentricity is consistent with the dissipation induced by a surface hydrocarbon ocean or disconnected seas (Sagan and Dermott, 1982; Dermott and Sagan, 1995; Sohl et al., 1995), a problem that itself has dissipated, given that a global surface hydrocarbon ocean is not present at Titan today. An internal ocean will also increase the tidal dissipation, by permitting greater flexing of the overlying ice shell (Sohl et al., 1995). Moreover, a warm and convecting ice shell would further amplify tidal dissipation (e.g. Sohl et al., 2003).

A cool Titan interior significantly diminishes the problem by limiting the interior dissipation within the ice shell (Tobie et al., 2005). Such could be consistent with an ice shell that is cool and conductive (Nimmo and Bills, 2010) or which is convecting sluggishly (Tobie et al., 2005). It is instead possible that Titan's eccentricity was excited in relatively recent geological time (Sohl et al., 1995; Bills and Nimmo, 2004). Models by Tobie et al. (2005) suggest that a relatively cool Titan, with a global ammonia–water ocean within, can have sufficiently low dissipation as to be consistent with Titan's present eccentricity having decayed from primordial, without need for recent excitation.

7. Implications for titan's geological and atmospheric evolution

7.1. Titan: Callisto with weather?

We propose that the satellite most akin to Titan is Callisto, with weather. In this scenario, Titan has been an endogenically relatively inactive world with a quiescent interior through much of its history. It is plausible that early in Solar System history Titan's radiogenic heat flux may have been great enough to trigger endogenic activity and perhaps somewhat amplified tidal dissipation; moreover, some amount of convection is expected during Titan's thermal evolution in order to lose its radiogenic heat while remaining incompletely differentiated. Analogous to Callisto's probable internal ocean (Spohn and Schubert, 2003), Titan's can be maintained by radiogenic heating given the pressure melting of ice along with available freezing point depressants, most notably ammonia (e.g. Sotin et al., 2009).

The preservation of large craters on Titan, at least some of which may be ancient, argues for a quiescent endogenic geological history. It is intriguing to compare portions of the Xanadu region on Titan (such as around 90°W, Fig. 11) to typical cratered terrain on Callisto. Might Titan have been a cratered landscape originally like Callisto that has been subsequently eroded principally by fluvial activity? There are many quasi-circular features in this region, which have some morphological characteristics of impact craters (e.g., central peaks, inward-facing scarps). If these features are impact craters, then eastern Xanadu represents an old surface subsequently eroded probably by fluvial activity. If eastern Xanadu is a region of degraded ancient cratered terrain, then this would have significant implications for Titan's history. Martian fluvially degraded cratered terrain still retains craters because fluvial activity largely ceased at the end of the heavy bombardment. For Titan to have such terrain and ongoing fluvial activity could imply one or more of at least three possible explanations: (1) alkane fluvial erosion on Titan is extremely inefficient relative to that by water on the Earth and Mars; (2) fluvial erosion very rarely occurs on some regions on Titan; and/or (3) it has started raining on Titan only in geologically recent times.

7.2. Titan's atmosphere

The chemical makeup of Titan's atmosphere is commonly cited as a chief reason to suspect endogenic activity at Titan, for two chief reasons. First, the lifetime of Titan's atmospheric methane against destruction by ultraviolet photolysis and high-energy charged particles in the upper atmosphere is only $\sim 10^7$–10^8 years, arguing for a replenishment source (e.g., Lunine and Atreya, 2008). Second, the Huygens Gas Chromatograph Mass Spectrometer (GCMS) measured radiogenically produced ^{40}Ar, the decay product of ^{40}K, which argues for some degree of communication between a rocky deep interior and the atmosphere, perhaps by ongoing outgassing via cryovolcanism (Niemann et al., 2005; Owen, 2005).

Hypotheses have been suggested for supplying Titan's methane-rich atmosphere that did not rely on cryovolcanic replenishment. McKay et al. (1993) considered that the warming sun may have been key to generating Titan's atmosphere over time. They

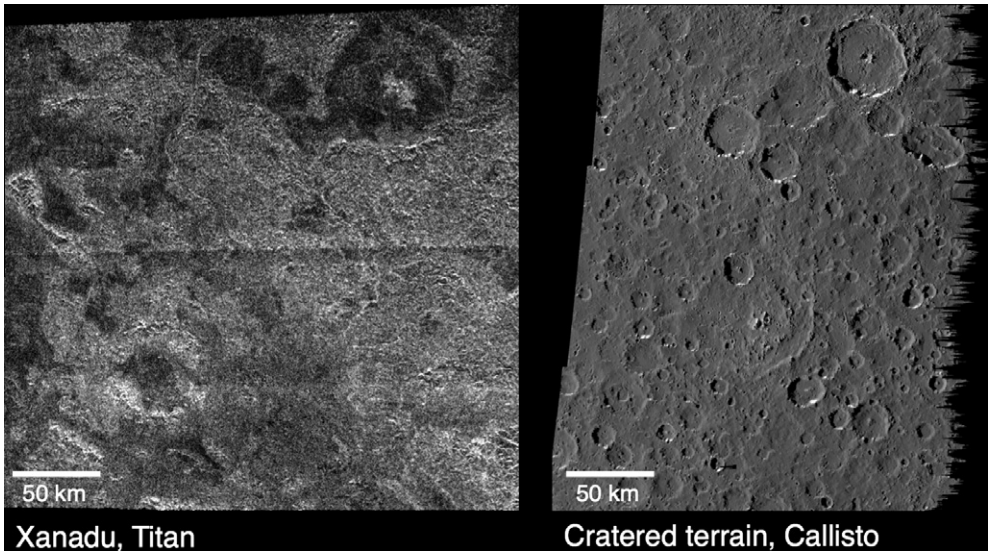

Fig. 11. A portion of the Xanadu region at Titan (left) compared to cratered terrain on Callisto (right), both shown to a common scale. Note the many quasi-circular features in Xanadu, which have some morphological characteristics of impact craters (e.g., central peaks and inward-facing scarps). If these features are impact craters, then Xanadu represents an old surface that has been subsequently eroded, probably by fluvial and aeolian activity. For comparison, the surface of Callisto is a substantially eroded cratered landscape, although the erosion mechanism is thought to be due to sublimation degradation (Moore et al., 2004). (Titan image is excerpted from Cassini radar swath T13, centered at ~10°S, 85°W; Callisto image is Galileo observation C9CSCRATER01 centered at ~6°S, 7°W.)

found that Titan might have experienced a Triton-like phase 3 Gyr ago, where Titan's surface may have been covered by methane and possibly nitrogen ice. The surface would have gradually warmed, releasing methane into the atmosphere, as the solar luminosity increased to the present day. Lorenz et al. (1997) concur that nitrogen may have been collapsed out of Titan's atmosphere in the past due to the faint young sun, and/or because ancient methane was photochemically destroyed at a rate faster than it could be supplied to the atmosphere. Gradual increase in solar luminosity and irradiation-induced lowering of the surface albedo may have released the frozen volatiles to the atmosphere over time.

Zahnle et al. (1992) and Griffith and Zahnle (1995) argued that Titan's atmosphere could be impact-generated, where low velocity impactors can deliver a volatile-rich atmosphere to early Titan while avoiding excess impact stripping. Supply of nitrogen is through the break-down of complex organic molecules and direct contribution of cometary nitrogen. (In this model, the only substantial difference between Titan and Callisto is that impact velocities are lower for impacts on Titan.) A corollary is that relatively recent large impacts into Titan (notably Menrva) can also contribute volatiles and/or liberate them from the interior. Kress and McKay (2004) note that large cometary impacts into Titan may indeed produce methane through catalysis by refractory dust. Zahnle (2010) suggests that the modest-sized impacts might saturate Titan's atmosphere with methane. In this way, it is plausible that impacts may have resupplied methane to Titan's atmosphere through time without cryovolcanism.

Titan's radiogenically produced ^{40}Ar does imply some degree of degassing from Titan's rocky interior. McKinnon (2010) finds that ~6% of Titan's total inventory of radiogenically produced ^{40}Ar has been degassed, and possibly ~10% if atmospheric loses are taken into account (Niemann et al., 2005). Either value is much more comparable to the degassing of Mars rather than the ~50% degassing of Earth. It might be possible that most ^{40}Ar degassing occurred very early in Titan's history, rather than through time via cryovolcanism, for example if Titan partially differentiated during a late heavy bombardment or through outgassing activity soon after. This permits the possibility that Titan experienced negligible outgassing throughout most of Solar System history, and today. However, very early degassing of Titan would imply a much greater fraction of the satellite must have been degassed to account for the present ^{40}Ar abundance, given that little of the ^{40}Ar production would have yet occurred through ^{40}K decay if degassing occurred very early. Another relevant issue is the possible incorporation of argon into clathrated ice, if water was present within Titan prior to ^{40}Ar release. It will be important to model the production and release of ^{40}Ar as coupled to impact bombardment and thermal evolution of Titan. This would allow a better understanding of whether significant cryovolcanism is necessary to explain Titan's ^{40}Ar budget, or whether early production and release is viable. It is worthwhile to revisit Titan's inferred atmospheric evolution within the premise that cryovolcanism may be minor or nonexistent on the satellite, and that exogenic processes have instead dominated the satellite's evolution.

8. Summary

Titan may be an exogenic world, with a landscape dominated by exogenic processes. Strong evidence exists for fluvial, lacustrine, aeolian, and impact processes on the surface. In contrast, evidence for endogenic cryovolcanism is equivocal at best. Moreover, Titan's tectonic structures may originate from external forcing and/or slow cooling and freezing of an interior ocean. The history of planetary exploration is rife with cautionary examples of planetary volcanism as misidentified in low resolution data, and shown instead to result from impact (e.g., the lunar Cayley Plains and icy satellite palimpsests) or tectonic processes (e.g., several of the icy satellites). Cryovolcanic interpretations of Tortola Facula and Ganesa Macula—which have been commonly cited as outstanding examples of cryovolcanism—do not remain credible upon examination of improved data. Moreover, features hypothesized to be formed by cryovolcanism at Hotei Regio may represent fluvial and lacustrine landforms instead. Overall the evidence for cryovolcanism is substantially short of compelling, and exogenic processes provide viable explanations for all features thus far suggested to by cryovolcanic.

Geophysical evidence supports a quiescent history for Titan's interior: impact crater morphologies suggest a low heat flux, it is probable that the interior is incompletely differentiated, gravity and global shape suggests that it is not currently convecting or significantly tidally heated, and a cool interior is most consistent with its orbital eccentricity and evolution. Titan's atmospheric chemistry is commonly cited as implying cryovolcanic replenishment of methane and venting of ^{40}Ar, but alternative scenarios for Titan's atmospheric evolution appear to be viable and warrant further investigation.

Titan may be most akin to Callisto with weather. Xanadu may represent an old surface that has been subsequently eroded, by fluvial and other processes. The hypothesis of Titan as a predominantly exogenic world can be tested through additional Cassini observations and analyses of putative cryovolcanic features, geophysical and thermal modeling of Titan's interior evolution, modeling of icy satellite landscape evolution that is shaped by exogenic processes alone, and consideration of possible means for supplying Titan's atmospheric constituents that do not rely on cryovolcanism. Interpreting Titan's landscape and the implications for Titan's history is both exciting and challenging, for its complexity and for the means we have to evaluate this landscape. Titan continues to be a complex and fascinating world.

Acknowledgments

We thank Amy Barr, Bruce Bills, Geoff Collins, Ken Edgett, Alan Howard, Krishan Khurana, Randy Kirk, Bill McKinnon, Giuseppe Mitri, Francis Nimmo, Conor Nixon, Flora Paganelli, Paul Schenk, Larry Soderblom, Christophe Sotin, Don Wilhelms, and Kevin Zahnle for valuable reviews and discussions on various aspects of this research. We are especially grateful for the formal reviews of Jani Radebaugh, Ellen Stofan, and an anonymous reviewer collectively whose comments substantially improved this report. We acknowledge Snowpacalypse 2010 for making the long-awaited completion of this paper possible. Funding for this work was provided by an Outer Planets Research Program grant (JMM) and the Cassini Project (RTP). The portion of this work performed by RTP was carried out at the Jet Propulsion Laboratory, California Institute of Technology, under a contract with the National Aeronautics and Space Administration.

References

Artemieva, N., Lunine, J.I., 2005. Impact cratering on Titan. II: Global melt, escaping ejecta, and aqueous alteration of surface organics. Icarus 175, 522–533.
Barnes, J.W. et al., 2006. Cassini observations of flow-like features in western Tui Regio, Titan. Geophys. Res. Lett. 33, L16204. doi:10.1029/2006GL026843.
Barnes, J.W. et al., 2007. Near infrared spectral mapping of Titan's mountains and channels. J. Geophys. Res. 112, E11006. doi:10.1029/2007JE002932.
Barr, A.C., Citron, R.I., Canup, R.M., 2010. Origin of a partially differentiated Titan. Icarus 209, 858–862. doi:10.1016/j.icarus.2010.05.028.
Bender, K.C., Rice, J.W., Wilhelms, D.E., Greeley, R., 1997. Geological map of Callisto. USGS Misc. Investigations Series, I-2581.
Bills, B.G., Nimmo, F., 2004. How does Titan retain a finite orbital eccentricity? Lunar Planet. Sci. XXXV. Abstract #1341.
Brown, R.H. et al., 2008. The identification of liquid ethane in Titan's Ontario Lacus. Nature 454, 607–610.
Burr, D.M., Emery, J.P., Lorenz, R.D., Collins, G.C., Carling, P.A., 2006. Sediment transport by liquid surficial flow: Application to Titan. Icarus 181, 235–242.
Burr, D.M. et al., 2008. The Titan wind tunnel: A new resource in the Planetary Aeolian Laboratory. Lunar Planet. Sci. 39. Abstract #2196.
Carr, M.H. et al., 1995. The Galileo Imaging Team plan for observing the satellites of Jupiter. J. Geophys. Res. 100, 18935–18955.
Chaikin, A., 2008. A Passion for Mars: Intrepid Explorers of the Red Planet. Abrams Inc., New York. pp. 55–57. 272pp.
Collins, G.C., 2005. Relative rates of fluvial bedrock incision on Titan and Earth. Geophys. Res. Lett. 32, L22202. doi:10.1029/2005GL024551.
Collins, G.C. et al., 2009. Tectonics of the outer planet satellites. In: Watters, T., Schultz, R. (Eds.), Planetary Tectonics. Cambridge Univ. Press, pp. 264–350.
Craddock, R.A., Howard, A.D., 2002. The case for rainfall on a warm, wet early Mars. J. Geophys. Res. 107, 5111, 21–36.
Croft, S.K., Kargel, J.S., Kirk, R.L., Moore, J.M., Schenk, P.M., Strom, R.G., 1995. Geology of Triton. In: Cruikshank, D.P., Matthews, M.S. (Eds.), Neptune and Triton. Univ. of Ariz. Press, Tucson, pp. 879–948.
Cutts, J.A., Soderblom, L.A., Sharp, R.P., Smith, B.A., Murray, B.C., 1971. The surface of Mars: 3. Light and dark markings. J. Geophys. Res. 76, 343–356.
Dermott, S.F., Sagan, C., 1995. Tidal effects of disconnected hydrocarbon seas on Titan. Nature 374, 238–240.
Drury, S., 2001. Image interpretation. Geology, third ed. Blackwell, Cheltenham, UK.
Elachi, C., 1988. Spaceborne Radar Remote Sensing: Applications and Techniques. IEEE Press, New York. 254pp.
Elachi, C. et al., 2004. RADAR: The Cassini Titan Radar Mapper. Space Sci. Rev. 115, 71–110.
Elachi, C. et al., 2005. Cassini radar views the surface of Titan. Science 308, 970–974.
Elachi, C. et al., 2006. Titan Radar Mapper observations from Cassini's T3 fly-by. Nature 441, 709–713.
Ezell, E.C., Ezell, L.N., 1984. On Mars: Exploration of the Red Planet 1958–1978. NASA SP-4212, pp. 175–192. 576pp.
Fagents, S.A., 2003. Considerations for effusive cryovolcanism on Europa: The post-Galileo perspective. J. Geophys. Res. 108, 5139. doi:10.1029/2003JE002128.
Farr, T.G., 1993. Radar interactions with geologic surfaces. In: Fulton, D. (Ed.), Guide to Magellan Image Interpretation. JPL Publication 93-24, pp. 45–56. <http://www.history.nasa.gov/JPL-93-24/jpl_93-24.htm>.
Ford, J.P. et al., 1989. In: Fulton, D. (Ed.), Spaceborne Radar Observations, a Guide for Magellan Radar-Image Analysis. JPL Publication 89-41.
Ford, J.P. et al., 1993. In: Fulton, D. (Ed.), Guide to Magellan Image Interpretation. JPL Publication 93-24.
Fortes, A.D., Grindrod, P.M., Trickett, S.K., Vocadlo, L., 2007. Ammonium sulfate on Titan: Possible origin and role in cryovolcanism. Icarus 188, 139–153.
Furfaro, R., Kargel, J.S., Lunine, J.I., Fink, W., Bishop, M.P., 2010. Identification of cryovolcanism on Titan using Fuzzy Cognitive Maps. Planet. Space Sci. 58 (5), 761–779. doi:10.1016/j.pss.2009.12.003.
Grasset, O., Sotin, C., Deschamps, F., 2000. On the internal structure and dynamics of Titan. Planet. Space Sci. 48, 617–636.
Greeley, R., 1971. Lunar Hadley Rille: Considerations of its origin. Science 172, 722–725.
Greeley, R., Chyba, C., Head, J.W., McCord, T., McKinnon, W.B., Pappalardo, R.T., 2004. Geology of Europa. In: Bagenal, F. et al. (Eds.), Jupiter: The Planet, Satellites & Magnetosphere. Cambridge Univ. Press, pp. 329–362.
Griffith, C.A., Zahnle, K., 1995. Influx of cometary volatiles to planetary Moons: The atmospheres of 1000 possible Titans. J. Geophys. Res. 100 (16), 907–916. 922.
Grindrod, P.M., Fortes, A.D., Nimmo, F., Feltham, D.L., Brodholt, J.P., Vocadlo, L., 2008. The long-term stability of a possible aqueous ammonium sulfate ocean inside Titan. Icarus 197, 137–151.
Hayes, A. et al., 2008a. Hydrocarbon lakes on Titan: Distribution and interaction with an isotropic porous regolith. Geophys. Res. Lett. 35, L09204. doi:10.1029/2008GRL033409.
Hayes, A.G. et al., 2008b. Joint analysis of Titan's surface using the Cassini VIMS and Radar instruments. Division for Planetary Sciences Annual Meeting, Ithaca. Abstract #34.06.
Hayes, A.G. et al., 2009. Observations and modeling of transient lacustrine features in Titan's South Polar Region. AGU Fall Meeting 2009. Abstract #P54C-02.
Head, J.W. et al., 2008. Volcanism on Mercury: Evidence from the first MESSENGER flyby. Science 321, 69–72.
Howard, A.D., Moore, J.M., Irwin, R.P., 2005. An intense terminal epoch of widespread fluvial activity on early Mars: 1. Valley network incision and associated deposits. J. Geophys. Res. 110, E12S14. doi:10.1029/2005JE002459.
Hueso, R., Sanchez-Lavega, A., 2006. Methane storms on Saturn's Moon Titan. Nature 442, 428–431.
Iess, L. et al., 2010. Gravity field, shape and moment of inertia of Titan. Science 327 (5971), 1367–1369. doi:10.1126/science.1182583.
Jaumann, R., Neukum, G., 2009. The surface age of Titan. Lunar Planet. Sci. 40. Abstract #1641.
Jaumann, R. et al., 2008. Fluvial erosion and post-erosional processes on Titan. Icarus 197, 526–538.
Jaumann, R. et al., 2009a. Geology and surface processes on Titan. In: Brown, R.H. et al. (Eds.), Titan from Cassini–Huygens. Springer, New York, pp. 75–140.
Jaumann, R. et al., 2009b. Icy satellites: Geological evolution and surface processes. In: Saturn after Cassini–Huygens. In: Dougherty, M. et al. (Eds.), Saturn from Cassini–Huygens. Springer, New York, pp. 637–682.
Johnson, T.V., 2005. Geology of the icy satellites. Space Sci. Rev. 116, 401–420.
Jones, K.B., Head, J.W., Pappalardo, R.T., Moore, J.M., 2003. Morphology and origin of palimpsests on Ganymede from Galileo observations. Icarus 164, 197–212.
Keller, H.U., Grieger, B., Küppers, M., Schröder, S.E., Skorov, Y.V., Tomasko, M.G., 2008. The properties of Titan's surface at the Huygens landing site from DISR observations. Planet. Space Sci. 56, 728–752.
Kirk, R.L. et al., 2009. Three-dimensional views of Titan's diverse surface features from Cassini radar stereogrammetry. Lunar Planet. Sci. 40, #1413.
Kirk, R.L. et al., 2010. La Sotra y las otras: Topographic evidence for (and against) cryovolcanism on Titan. AGU Fall Meeting 2010. Abstract # P22A-03.
Korycansky, D.G., Zahnle, K.J., 2005. Modeling crater populations on Venus and Titan. Planet. Space Sci. 52, 695–710.
Kress, M.E., McKay, C.P., 2004. Formation of methane in comet impacts: Implications for Earth, Mars, and Titan. Icarus 168, 475–483.
Le Corre, L. et al., 2009. Analysis of a cryolava flow-like feature on Titan. Planet. Space Sci. 57, 870–879.

Leighton, R.B. et al., 1969a. Mariner 6 television pictures: First report. Science 165, 684–690.
Leighton, R.B. et al., 1969b. Mariner 7 television pictures: First report. Science 165, 787–795.
Leighton, R.B. et al., 1969c. Mariner 6 and 7 television pictures: Preliminary analysis. Science 166, 49–67.
Lopes, R.M.C. et al., 2007. Cryovolcanic features on Titan's surface as revealed by the Cassini Titan Radar Mapper. Icarus 186, 395–412.
Lopes, R.M.C. et al., 2010. Distribution and interplay of geologic processes on Titan from Cassini radar data. Icarus 205, 540–558.
Lorenz, R.D., 2005. Titan's methane monsoon: Evidence of catastrophic hydrology from Cassini RADAR. Bull. Am. Astron. Soc. DPS 37 (3). Abstract #53.07.
Lorenz, R.D., Radebaugh, J., 2009. Global pattern of Titan's dunes: Radar survey from the Cassini prime mission. Geophys. Res. Lett. 36, L03202. doi:10.1029/2008GL036850.
Lorenz, R.D., McKay, C.P., Lunine, J.I., 1997. Photochemically driven collapse of Titan's atmosphere. Science 275, 642–644.
Lorenz, R.D., Griffith, C.A., Lunine, J.I., McKay, C.P., Rennò, N.O., 2005. Convective plumes and the scarcity of Titan's clouds. Geophys. Res. Lett. 32, L01201. doi:10.1029/2004GL021415.
Lorenz, R.D. et al., 2006. The sand seas of Titan: Cassini RADAR observations of longitudinal dunes. Science 312, 724–727.
Lorenz, R.D. et al., 2008. Fluvial channels on Titan: Initial Cassini RADAR observations. Planet. Space Sci. 56, 1132–1144.
Lucchita, B.K., Soderblom, L.A., 1982. The geology of Europa. In: Morrison, D. (Ed.), Satellites of Jupiter. Univ. of Ariz. Press, Tucson, pp. 521–555.
Lunine, J.I., Atreya, S.K., 2008. The methane cycle on Titan. Nat. Geosci. 1, 159–164.
Malin, M.C., 1978. Surfaces of Mercury and the Moon: Effects of resolution and lighting conditions on the discrimination of volcanic features. Proc. Lunar Sci. Conf. 9, 3395–3409.
McKay, C.P., Pollack, J.B., Lunine, J.I., Courtin, R., 1993. Coupled atmosphere–ocean models of Titan's past. Icarus 102, 88–98.
McKinnon, W.B., 1997. NOTE: Mystery of Callisto: Is it undifferentiated? Icarus 130, 540–543. doi:10.1006/icar.1997.5826.
McKinnon, W.B., 2006. On convection in ice I shells of outer Solar System bodies, with detailed application to Callisto. Icarus 183, 435–450.
McKinnon, W.B., 2010. Argon-40 degassing from Titan and Enceladus: A tale of two satellites. Lunar Planet. Sci. 41. Abstract #2718.
Melosh, H.J., 1982. A simple mechanical model of Valhalla basin, Callisto. J. Geophys. Res. 87 (B3), 1880–1890. doi:10.1029/JB087iB03p01880.
Mitri, G., Showman, A.P., Lunine, J.I., Lorenz, R.D., 2007. Hydrocarbon lakes on Titan. Icarus 186, 385–394.
Mitri, G., Showman, A.P., Lunine, J.I., Lopes, R.M.C., 2008. Resurfacing of Titan by ammonia–water cryomagma. Icarus 196, 216–224.
Mitri, G., Pappalardo, R.T., Stevenson, D.J., 2009. Is Titan partially differentiated? Eos Trans. AGU 90 (52) (Fall Suppl.). Abstract P43F-07.
Mitri, G. et al., 2010a. Mountains on Titan: Modeling and observations. J. Geophys. Res. 115, E10002. doi:10.1029/2010JE003592.
Mitri, G., Pappalardo, R.T., Stevenson, D.J., 2010b. Evolution and interior structure of Titan. Lunar Planet. Sci. 41. Abstract #2229.
Moore, J.M., Howard, A.D., 2010. Are the basins of Titan's Tui Regio and Hotei Regio sites of former low latitude seas? Geophys. Res. Lett. 37, L22205. doi:10.1029/2010GL045234.
Moore, J.M. et al., 2004. Callisto. In: Bagenal, F. et al. (Eds.), Jupiter: The Planet, Satellites, and Magnetosphere. Cambridge Univ. Press, New York, pp. 397–426.
Moore, J.M., Howard, A.D., Schenk, P.M., Pappalardo, R.T., 2010. Titan: Can fluvial erosion patterns tell us anything about initial landforms and regional landscapes? Lunar Planet. Sci. 41. Abstract #1167.
Mosqueira, I., Estrada, P.R., 2009. The Ganymede, Titan, Callisto, Iapetus trend: Interpretation of Titan's moment of inertia. Eos Trans. AGU 90 (52) (Fall Suppl.). Abstract P43F-08.
Muehlberger, W.R., Ulnch, G.E., 1981. Summary of geologic results from Apollo 16. In: Ulrich, G.E. (Ed.), Geology of the Apollo 16 Area, Central Lunar Highlands. US Geol. Surv. Prof. Pap. 1048, pp. 1–5.
Murchie, S.L., Head, J.W., Plescia, J.B., 1990. Tectonic and volcanic evolution of dark terrain and its implications for the internal structure of Ganymede. J. Geophys. Res. 95, 10743–10768.
Murray, B.C., Soderblom, L.A., Sharp, R.P., Cutts, J.A., 1971. The surface of Mars 1. Cratered terrains. J. Geophys. Res. 76 (2), 313–330.
Murray, B.C. et al., 1974. Mercury's surface: Preliminary description and interpretation from Mariner 10 pictures. Science 185, 169–179.
Murray, B.C., Strom, R.G., Trask, N.J., Gault, D.E., 1975. Surface history of Mercury – Implications for terrestrial planets. J. Geophys. Res. 80, 2508–2514.
Neish, C.D. et al., 2006. The potential for prebiotic chemistry in the possible cryovolcanic dome Ganesa Macula on Titan. Int. J. Astrobiol. 5 (1), 57–65. doi:10.1017/S1473550406002898.
Nelson, R.M. et al., 2009a. Photometric changes on Saturn's Titan: Evidence for active cryovolcanism. Geophys. Res. Lett. 36, L04202. doi:10.1029/2008GL036206.
Nelson, R.M. et al., 2009b. Saturn's Titan: Surface change, ammonia, and implications for atmospheric and tectonic activity. Icarus 199, 429–441.
Niemann, H.B. et al., 2005. The abundances of constituents of Titan's atmosphere from the GCMS instrument on the Huygens probe. Nature 438, 779–784.
Nimmo, F., Bills, B.G., 2010. Shell thickness variations and the long wavelength topography of Titan. Icarus 208, 896–904.
Ori, G.G., Marinangeli, L., Baliva, A., Bressan, M., Strom, R.G., 1998. Fluid dynamics of liquids on Titan's surface. Planet. Space Sci. 46, 1417–1421.
Owen, T., 2005. Huygens rediscovers Titan. Nature 438, 756–757.
Paganelli, F. et al., 2005. Channels and fan-like features on Titan's surface imaged by the Cassini RADAR. Proc. Lunar Sci. Conf. 36. Abstract #2150.
Paganelli, F. et al., 2010. Preliminary analysis of structural elements of Titan and implications for stress. Lunar Planet. Sci. 41. Abstract #2664.
Pappalardo, R.T. et al., 1998. Geological evidence for solid-state convection in Europa's ice shell. Nature 391, 365–368.
Pappalardo, R.T. et al., 2004. Geology of Ganymede. In: Bagenal, F. et al. (Eds.), Jupiter: The Planet, Satellites & Magnetosphere. Cambridge Univ. Press, New York, pp. 363–396.
Parker, G., 2005. Comparative application of dimensionless bankfull hydraulic relations for Earth and Titan. American Geophysical Union Fall Meeting 2005. Abstract #H31G-06.
Passey, Q.R., Shoemaker, E.M., 1982. Craters and basins on Ganymede and Callisto: Morphological indicators of crustal evolution. In: Morrison, D. (Ed.), Satellites of Jupiter. Univ. of Arizona Press, Tucson, AZ, pp. 379–434.
Perron, J.T., Lamb, M.P., Coven, C.D., Fung, I.Y., Yager, E., Ádámkovicks, M., 2006. Valley formation and methane precipitation rates on Titan. J. Geophys. Res. 111, E11001. doi:10.1029/2005JE02602.
Porco, C.C. et al., 2005. Imaging of Titan from the Cassini spacecraft. Nature 434, 159–168.
Prockter, L.M., 2004. Ice volcanism on Jupiter's Moons and beyond. In: Lopes, R.M.C., Gregg, T.K.P. (Eds.), Volcanic Worlds: Exploring the Solar System's Volcanoes. Springer-Verlag, Berlin, pp. 145–177.
Prockter, L.M., Figueredo, P., Pappalardo, R.T., Head III, J.W., Collins, G.C., 2000. Geology and mapping of dark terrain on Ganymede and implications for grooved terrain formation. J. Geophys. Res. 105, 22519–22540.
Radebaugh, J. et al., 2007a. Dunes on Titan observed by Cassini Radar. Icarus 194, 690–703.
Radebaugh, J. et al., 2007b. Mountains on Titan observed by Cassini Radar. Icarus 192, 77–91.
Radebaugh, J. et al., 2010. Regional geomorphology and history of Titan's Xanadu province. Icarus 211, 1, 672–685.
Ray, R.G., 1960. Aerial Photographs in Geologic Interpretation and Mapping. Geological Survey Professional Paper 373. US Gov. Printing Office, Washington.
Robinson, M.S., Lucey, P.G., 1997. Recalibrated Mariner 10 color mosaics: Implications for mercurian volcanism. Science 275, 197–200.
Robinson, M.S., Tanaka, K.L., 1990. Magnitude of a catastrophic flood event at Kasei Valles, Mars. Geology 18, 902–905.
Robinson, M.S. et al., 2008. Reflectance and color variations on Mercury: Regolith processes and compositional heterogeneity. Science 321, 66–69.
Rodriguez, S. et al., 2006. Cassini/VIMS hyperspectral observations of the Huygens landing site on Titan. Planet. Space Sci. 54, 1510–1523.
Rubin, D.M., Hesp, P.A., 2009. Multiple origins of linear dunes on Earth and Titan. Nat. Geosci. 2, 653–658.
Sagan, C., Dermott, S.F., 1982. The tide in the seas of Titan. Nature 300, 731–733.
Schaller, E.L., Roe, H.G., Schneider, T., Brown, M.E., 2009. Storms in the tropics of Titan. Nature 460, 873–875.
Schenk, P.M., Moore, J.M., 1995. Volcanic constructs on Ganymede and Enceladus: Topographic evidence from stereo images and photoclinometry. J. Geophys. Res. 100, 19009–19022.
Schenk, P.M., Moore, J.M., 1998. Geologic landforms and processes on icy satellites. In: Schmitt, B. et al. (Eds.), Solar System Ices. Kluwer, Boston, pp. 551–578.
Schenk, P.M., McKinnon, W.B., Gwynn, D., Moore, J.M., 2001. Flooding of Ganymede's bright terrains by low-viscosity water–ice lavas. Nature 410, 57–60.
Schenk, P., Chapman, C., Zahnle, K., Moore, J., 2004. Ages and interiors: The cratering record of the Galilean satellites. In: Bagenal, F. et al. (Eds.), Jupiter: The Planet, Satellites & Magnetosphere. Cambridge Univ. Press, pp. 427–456.
Schubert, G., Anderson, J.D., Spohn, T., McKinnon, W.B., 2004. Interior composition, structure, and dynamics of the Galilean satellites. In: Bagenal, F. et al. (Eds.), Jupiter: The Planet, Satellites & Magnetosphere. Cambridge Univ. Press, pp. 281–306.
Sharp, R.P., Murray, B.C., Leighton, R.B., Soderblom, L.A., Cutts, J.A., 1971a. The surface of Mars: 4. South polar cap. J. Geophys. Res. 76, 357–368.
Sharp, R.P., Soderblom, L.A., Murray, B.C., Cutts, J.A., 1971b. The surface of Mars: 2. Uncratered terrains. J. Geophys. Res. 76, 331–342.
Shoemaker, E.M., Lucchitta, B.K., Plescia, J.B., Squyres, S.W., Wilhelms, D.E., 1982. The geology of Ganymede. In: Morrison, D. (Ed.), Satellites of Jupiter. Univ. of Ariz. Press, Tucson, pp. 435–520.
Sklar, L.S., Polito, P., Zygielbaum, B., Collins, G.C., 2008. Abrasion susceptibility of ultra-cold water ice: Preliminary measurements of abrasion rate, tensile strength and elastic modulus. Lunar Planet. Sci. 39. Abstract #9076.
Soderblom, L.A. et al., 2007a. Correlations between Cassini VIMS spectra and RADAR SAR images: Implications for Titan's surface composition and the character of the Huygens probe landing site. Planet. Space Sci. 55, 2025–2036.
Soderblom, L.A. et al., 2007b. Topography and geomorphology of the Huygens landing site on Titan. Planet. Space Sci. 55, 2015–2024.
Soderblom, L.A. et al., 2009. The geology of Hotei Regio, Titan: Correlation of Cassini VIMS and RADAR. Icarus 204, 610–618.
Sohl, F., Sears, W.D., Lorenz, R.D., 1995. Tidal dissipation on Titan. Icarus 115, 278–294.
Sohl, F., Hussmann, H., Schwentker, B., Spohn, T., Lorenz, R.D., 2003. Interior structure models and tidal Love numbers of Titan. J. Geophys. Res. 108, 5130. doi:10.1029/2003JE002044.
Solomon, S.C. et al., 2001. The MESSENGER mission to Mercury: Scientific objectives and implementation. Planet. Space Sci. 49, 1445–1465.

Sotin, C. et al., 2005. Release of volatiles from a possible cryovolcano from near-infrared imaging of Titan. Nature 435, 786–789.
Sotin, C., Mitri, G., Rappaport, N., Schubert, G., Stevenson, D., 2009. Titan's interior structure. In: Brown, R.H. et al. (Eds.), Titan from Cassini–Huygens. Springer, New York, pp. 61–73.
Spencer, J. et al., 2009. Enceladus: An active cryovolcanic satellite. In: Dougherty, M. et al. (Eds.), Saturn from Cassini–Huygens. Springer, New York, pp. 683–724.
Spohn, T., Schubert, G., 2003. Oceans in the icy Galilean satellites of Jupiter? Icarus 161, 456–467.
Spudis, P., 1984. Apollo 16 site geology ad impact melts: Implications for the geologic history of the lunar highlands. Proc. Lunar. Sci. Conf., Part 1, J. Geophys. Res. 89 (Suppl.), C95–C107.
Squyres, S.W., Croft, S.K., 1986. The tectonics of icy satellites. In: Burns, J.A., Matthews, M.S. (Eds.), Satellites. Univ. of Arizona Press, Tucson, pp. 293–341.
Squyres, S.W., Reynolds, R.T., Cassen, P.M., Peale, S.J., 1983a. Liquid water and active resurfacing on Europa. Nature 301, 225–226.
Squyres, S.W., Reynolds, R.T., Cassen, P.M., Peale, S.J., 1983b. The evolution of Enceladus. Icarus 53, 319–331.
Stefan, K. et al., 2010. Specular reflection on Titan: Liquids in Kraken Mare. Geophys. Res. Lett.. doi:10.1029/2009GL042312.
Stevenson, D., 1982. Volcanism and igneous processes in small icy satellites. Nature 298, 142–144.
Stiles, B.W. et al., 2009. Determining Titan surface topography from Cassini SAR data. Icarus 202, 584–598.
Stofan, E.R. et al., 2006. Mapping of Titan: Results from the first Titan radar passes. Icarus 185, 443–456.
Stofan, E.R. et al., 2007. The lakes of Titan. Nature 445, 61–64.
Strom, R.G., Trask, N.J., Guest, J.E., 1975. Tectonism and volcanism on Mercury. J. Geophys. Res. 80, 2478–2507.
Thomas, P.J., Squyres, S.W., 1990. Formation of crater palimpsests on Ganymede. J. Geophys. Res. 95, 19161–19174.
Tobie, G., Grasset, O., Lunine, J.I., Mocquet, A., Sotin, C., 2005. Titan's internal structure inferred from a coupled thermal–orbital model. Icarus 175, 496–502.
Tobie, G., Lunine, J.I., Sotin, C., 2006. Episodic outgassing as the origin of atmospheric methane on Titan. Nature 440, 61–64.
Trask, N.J., Guest, J.E., 1975. Preliminary geologic terrain map of Mercury. J. Geophys. Res. 80, 2461–2477.
Turtle, E.P., Perry, J.E., McEwen, A.S., Del Genio, A.D., Barbara, J., West, R.A., Dawson, D.D., Porco, C.C., 2009. Cassini imaging of Titan's high-latitude lakes, clouds, and southpolar surface changes. Geophys. Res. Lett. 36, L02204. doi:10.1029/2008GL036186.
Wall, S.D. et al., 2009. Cassini RADAR images at Hotei Arcus and Western Xanadu, Titan: Evidence for geologically recent cryovolcanic activity. Geophys. Res. Lett. 36, L04203. doi:10.1029/2008GL036415.
Wall, S. et al., 2010. Active shoreline of Ontario Lacus, Titan: A morphological study of the lake and its surroundings. Geophys. Res. Lett. 37, L05202. doi:10.1029/2009GL041821.
Wilhelms, D.E., 1970. Summary of lunar stratigraphy—Telescopic observations. US Geol. Survey Prof. Paper 599-F.
Wilhelms, D.E., 1976. Mercurian volcanism questioned. Icarus 28, 551–558.
Wilhelms, D.E., 1993. To a Rocky Moon: A Geologist's History of Lunar Exploration. University of Arizona Press, Tucson, AZ, 477pp.
Wood, C.A., Lorenz, R., Kirk, R., Lopes, R., Mitchell, K., Stofan, E., 2010. Impact craters on Titan. Icarus 206, 334–344.
Zahnle, K., 2010. Titan's impact history. Titan through Time. Abstract for Titan through Time Workshop, NASA Goddard Space Flight Center, Green Belt, MD.
Zahnle, K., Pollack, J.B., Grinspoon, D., Dones, L., 1992. Impact-generated atmospheres over Titan, Ganymede, and Callisto. Icarus 95, 1–23.
Zebker, H.A., Stiles, B., Hensley, S., Lorenz, R., Kirk, R.L., Lunine, J., 2009. Size and shape of Saturn's Moon Titan. Science 324, 921–923.
Zhong, F., Mitchell, K.L., Hays, C.C., Choukroun, M., Barmatz, M., Kargel, J.S., 2009. The rheology of cryovolcanic slurries: Motivation and phenomenology of methanol–water slurries with implications for Titan. Icarus 202, 607–619.